Anti-inflammatory activities and the underlying mechanisms of fisetin, quercetin, and myricetin

by

Ruting ZHONG

SUPERVISOR: Chengwei HE

CO-SUPERVISOR: Jianbo XIAO

Master of Philosophy

in

Chinese Medicinal Science

2022

Institute of Chinese Medical Sciences

University of Macau

非瑟酮、槲皮素和楊梅素的抗炎活性及其作用機製

鐘汝婷

指導老師：何承偉

第二指導老師：肖建波

哲学碩士（中藥學）

2022

中華醫藥研究院

澳門大學

Declaration

I declare that the thesis here submitted is original except for the source materials explicitly acknowledged and that this thesis as a whole or any part of this thesis has not been previously submitted for the same degree or for a different degree.

I also acknowledge that I have read and understood the Rules on Handling Student Academic Dishonesty and the Regulations of the Student Discipline of the University of Macau.

Signature:_____

Date:_____

Acknowledgements

The two-year postgraduate career is fleeting, and I feel very grateful by this study journey. I want to express my sincere gratitude to many people who helped me along the way.

I would like to express the deepest gratitude to my supervisors, Prof. Chengwei He and Prof. Jianbo Xiao for their guidance, care, and efforts over my entire master study. I am very moved by Prof. He for his huge support and care for me. His kindness has deeply touched me. He gave me many professional and meticulous guidance in my scientific research and PhD application. Also, I feel very appreciated for the opportunities Prof. Xiao gave to me. His hard-working and enterprising qualities inspired me a lot to study hard.

Then, a special thank comes to my senior colleague, Mrs. Lingchao Miao, who helped me a lot in designing my cell experiment and teaching me many biological experimental skills. Also, many thanks to Ms. Lihua Tan, Dr. Yanbei Tu, Mr. Zhimin Miao, Ms. Haolin Zhang for their help and encouragement in my master study.

In addition, I am very lucky and happy to study in two lovely teams including the members of Dr. Yanbei Tu, Ms. Lihua Tan, Dr. Haiyong Wang, Ms. Yuxin Zhao, Mr. Zhimin Miao, Ms. Jinmiao Zhong; Mrs. Lingchao Miao, Ms. Haolin Zhang, Ms. Xiaomei Lv, Mr. Ruiwei Xie, Ms. Mingxin Zhang. They are all kind and responsible.

Moreover, I want to thanks for the Macao Science and Technology Development Fund and the Research Found of the University of Macau for my financial support in my master study. And thanks for the efforts of lab technicians.

Last but not least, I am very appreciated for my family members and good friend for their kindest care, greatest support and love.

Abstract

Fisetin, quercectin, and myricetin are flavonols with similar structure but different number of hydroxyl groups. The present research focused on the anti-inflammatory activities and the underlying mechanisms of fisetin, quercetin, and myricetin. *In vitro* experiment showed that the number of hydroxyl group in flavonols obviously affects their anti-inflammation activity in lipopolysaccharide-stimulated RAW264.7 cells. Among flavonols in safe concentrations, they suppressed the overproduction of nitric oxide, and fisetin showed the best activity with an inhibition rate of 52% at 20 μM. These flavonols reduced the expression levels of ROS, TNF-α, and IL-6 with variable effects. And they could block the activation of NF-κB and MAPK pathways by partially suppressing levels of phosphorylation of IκBα, p65, JNK, ERK, MEK, and reducing the nuclear translocation of NF-κB p65. In addition, several degradation products of fisetin were formed by methylation and glucuronidation. And quercetin and myricetin were transformed into several new products, including methylated quercetin and methylated myricetin, respectively. According to the comparative result, fisetin is an excellent anti-inflammatory reagent. Therefore, *in vivo* research was conducted to test whether fisetin has the liver protective and anti-inflammatory effects in D-GalN/LPS-induced acute liver injury from C57BL/6 mice. Results indicated that the pretreatment of fisetin could suppress the levels of AST, ALT, IL-1β, IL-6, and TNF-α in serum and reduced the MDA and CAT levels in hepatic tissues. In macroscopic view and H&E staining analysis, fisetin pretreatment reduced hepatic congestion, liver necrosis, and inflammatory cell infiltration. The underlying mechanism of this hepatoprotective effect was possibly associated with NF-κB signaling pathway. Thus, fisetin, quercetin, and myricetin are three potential agents again inflammation and among which fisetin showed the excellent effect. Fisetin may be a promising agent for the treatment of acute liver injury.

Keywords: Fisetin; Quercectin; Myricetin; Anti-inflammation; RAW264.7; Acute liver injury; D-GalN; LPS

摘要

非瑟酮、槲皮素和楊梅素是結構相似但羥基數不同的黃酮醇。本研究旨在探討非瑟酮、槲皮素和楊梅素的抗炎活性及其潛在機製。體外實驗表明，黃酮醇的羥基數目明顯影響其在脂多糖刺激的 RAW264.7 細胞中的抗炎活性。在安全濃度下，它們均能抑製一氧化氮的過量產生，其中非瑟酮顯示出最好的抑製效果，在 20 μM 時抑製率達 52%。三種黃酮醇均不同程度地降低了 ROS、TNF-α和 IL-6 的表達水平。它們通過部分抑製 IκBα、p65、JNK、ERK、MEK 的磷酸化水平和減少 NF-κB p65 的核轉移來阻斷 NF-κB 和 MAPK 通路的激活。此外，非瑟酮在細胞內降解為甲基化和葡萄糖醛酸化產物，槲皮素和楊梅素分別轉化為甲基化槲皮素和甲基化楊梅素等新產物。經過對比，非瑟酮是一種良好的抗炎物質。因此，研究選用非瑟酮進行後續體內研究，探究其是否對 D-GalN/LPS 誘導的 C57BL/6 小鼠急性肝損傷有肝臟保護和抗炎作用。結果表明，非瑟酮預處理可以抑製血清中 AST、ALT、IL-1β、IL-6 和 TNF-α的水平，降低肝組織中 MDA 和 CAT 的水平。在觀察肝臟組織和 H&E 染色分析中，非瑟酮預處理減少了肝充血、肝壞死和炎性細胞浸潤現象。這種肝臟保護活性的潛在機製可能與 NF-κB 信號通路有關。綜上所述，非瑟酮、槲皮素和楊梅素是三種潛在的抗炎成分，其中非瑟酮表現出更好的活性。非瑟酮預處理可能是治療 D-GalN/LPS 刺激引起急性肝損傷的一種前景藥物。

關鍵字：非瑟酮；槲皮素；楊梅素; 抗炎; RAW264.7；急性肝損傷; D-半乳糖胺；脂多糖

Table of Contents

List of Tables and Figures

List of Abbreviations

LPS	Lipopolysaccharide
NO	Nitric oxide
ROS	Reactive oxygen species
IL-6	Interleukin-6
TNF-α	Tumor necrosis factor-alpha
iNOS	Inducible NO synthase
NF-κB	Nuclear factor-κB
MAPK	Mitogen activated protein kinase
JNK	c-Jun NH2-terminal kinase
ERK	Extracellular signal-regulated kinase
MEK	Mitogen-activated protein kinase
Fis	Fisetin
Que	Quercetin
Myr	Myricetin
DMSO	Dimethyl sulfoxide
DCFH-DA	Dichlorodihydro-fluorescein diacetate
MTT	3-(4, 5-dimethylthiazol-2-yl)-2, 5-diphenyltetrazolium bromide
DMEM	Dulbecco's Modified Eagle Medium
FBS	Fetal bovine serum
PBS	Phosphate-buffered saline
PMSF	Phenylmethylsulfonyl fluoride
TBST	Tris-Buffered Saline/Tween
DAPI	4',6-diamidino-2-phenylindole
D-GalN	D-galactosamine

AST	Aspartate aminotransferase
ALT	Alanine aminotransferase
CAT	Catalase
MDA	Malondialdehyde
H & E	Hematoxylin-eosin
PVDF	Polyvinylidene fluoride
ELISA	Enzyme Linked Immune Sorbent Assay

Chapter 1 Introduction

Inflammation is a kind of physical responses in immune system that protects human bodies against tissue injury or infection (Hu et al., 2019). Inflammatory response under normal condition has protective effects on body functions, but it would cause host injury when lacking control (Ayala et al., 2019). Chronic inflammatory diseases have been reported to associated with rheumatoid arthritis (Tu et al., 2019), cardiovascular disease (Furman et al., 2019), and Alzheimer's disease (Qian et al., 2021). Regarding for acute inflammatory diseases, acute liver injury (ALI) is a severe disease characterized by sudden failure of liver function, which were mainly caused by autoimmunity, virus infection, toxic substance ingestion, and so on (Stravitz and Lee, 2019). ALI has high mortality rate and poor prognosis with complex mechanisms, which macrophages play an important role (Linde et al., 2007). Thus, the safe and effective pretreatment therapy is important for ALI. Lipopolysaccharides (LPS), a kind of endogenous gut-derived bacterial, is a main endotoxin in the process of liver damage. D-galactosamine (D-GalN) can induce the ALI in just a few hours. The combination of D-GalN with LPS can trigger ALI symptom like human bodies (Wu et al., 2019), which are characterized by hepatic necrosis, inflammation, and oxidative stress (Liu et al., 2015).

RAW264.7 macrophage is an important immune cell and plays a pivotal role during inflammation in host defenses against pathogens infection. When RAW264.7 cells induce by lipopolysaccharide (LPS), an endotoxin widely used in inflammation models, they will promote inflammatory responses by producing nitric oxide (NO) and reactive oxygen species (ROS) levels, and generating pro-inflammatory mediators such as interleukin-6 (IL-6), tumor necrosis factor-alpha (TNF-α), and inducible NO synthase (iNOS), recruiting other immune cells to the site of damage infection (Lim et al., 2021; C. Tian et al., 2021). Several signaling pathways were demonstrated to closely associate with inflammation in LPS-induced RAW264.7 cells. A transcriptional regulator nuclear factor-κB (NF-κB) is vitally involved in the pathogenesis of various inflammatory diseases, which modulates the production of many cytokines and mediators (Tak and Firestein, 2001). Besides, NF-κB could be activated through mitogen activated protein kinase (MAPK) such as c-Jun NH2-

terminal kinase (JNK), extracellular signal-regulated kinase (ERK), and mitogen-activated protein kinase (MEK) (Buchanan et al., 2010; Huang et al., 2012).

Dietary flavonols are typical and promising phytochemicals belonging to the flavonoids. They have been recognized to exert various effects such as anti-oxidant, anti-microbial, anti-cancer, anti-inflammatory, and so on (Barreca et al., 2021; Wang et al., 2006). Fisetin (3,3′,4′,7-tetrahydroxyflavone), quercetin (3,3',4',5,7-pentahydroxyflavone), and myricetin (3,3′,4′,5,5′,7-hexahydroxyflavone) are three structural related flavonols with flavon-3-ol (**Fig. 2.1A**). Fisetin is widely found in strawberry, onion, and grape from 2 to 160 μg/g (Arai et al., 2000). Quercetin is a major flavonoid of many fruits and vegetables such as mango, apple and tea (Kandemir et al., 2022). Also, myricetin is distributed in many foods including berry, onion, and red wine (Häkkinen et al., 1999). Different structures of polyphenols were observed to have various pharmacological activities, absorption, metabolism (Hollman, 2004; Y. Tian et al., 2021). However, there is no comparative and systematic research on the anti-inflammatory effect and metabolism condition of fisetin, quercetin, and myricetin. Therefore, the present work was focused on anti-inflammatory potential with their underlying mechanisms and metabolic situation of structural related flavonols on LPS-induced RAW264.7 macrophages model, and the anti-inflammatory effect on the pretreatment of fisetin against acute liver injury on D-GalN/LPS-stimulated acute liver injury.

Chapter 2 Anti-inflammatory activities and the underlying mechanisms on RAW264.7 macrophages of fisetin, quercetin, and myricetin

2.1 Materials and Methods

2.1.1 Chemicals and reagents

Lipopolysaccharide (LPS) from Escherichia coli O111:B4, dimethyl sulfoxide (DMSO), and Griess reagent were purchased from Sigma Aldrich (St. Louis, MO, USA). Dichlorodihydro-fluorescein diacetate (DCFH-DA) probe (S0033S) and 3-(4, 5-dimethylthiazol-2-yl)-2, 5-diphenyltetrazolium bromide (MTT) were obtained from Beyotime Biotechnology (Shanghai, China). Penicillin-streptomycin (P/S), Dulbecco's Modified Eagle Medium (DMEM/high glucose), fetal bovine serum (FBS), and phosphate-buffered saline (PBS) were purchased from Gibco (Carlsbad, CA, USA). Primary antibodies against iNOS, JNK, ERK, MEK, IκBα, NFκB p65, phosphorylated (p)- JNK, p-ERK, p-MEK, p-IκBα, p-p65, GAPDH, Lamin B, and the secondary antibody were acquired from Cell Signaling Technology (Danvers, MA, United States). Tumour necrosis factor-α (TNF-α) and interleukin-6 (IL-6) ELISA kits were obtained from Neobioscience Technology Co., Ltd (Shenzhen, China). Fisetin, quercetin, and myricetin were purchased from Tokyo Chemical Industry Co., Ltd. The HPLC purity of them was $\geqslant$ 97.0%.

2.1.2 Cell culture and flavonols treatment

A mouse macrophage cell line RAW264.7 was purchased from the American Type Culture Collection (ATCC, VA, USA). The RAW264.7 cells were cultured in DMEM/High Glucose with 1% P/S (v/v) and 10% (v/v) FBS and maintained in the atmosphere of 95% humidity and 5% CO_2 at 37 °C. The cells were sub-cultured into a new 50 cm2 flask (Thermo Fisher Scientific, MA, USA) when they reached 80% confluence. Fisetin, quercetin, and myricetin were dissolved in DMSO to yield stock solutions of 100 mM and stored at -20 ºC. Then they freshly diluted with DMEM with

10% FBS to make working solutions, which the concentrations of DMSO were less than 0.1%.

2.1.3 Cytotoxicity assay

Cell viability was detected by MTT method with a few modifications (Miao et al., 2019). RAW 264.7 cells (1×10^4 cells/well) were seeded into 96-well plates and adhered overnight. Then, the cells were treated with DMEM or increasing concentrations of flavonols (fisetin at 5, 10, and 20 μM; quercetin at 10, 20, and 40 μM; myricetin at 20, 40, 80 μM) for 24 h. Then, the supernatant was removed and 100 μL solution of MTT (10 mg/ml) with flesh DMEM (MTT: DMEM = 1: 10) was added to each well, incubating at 37 °C for 3 h. Thereafter, the MTT media were carefully replaced with 150 μl DMSO for dissolving the formazan crystals. After shaking for 30 min, the absorbance at 490 nm was read through a microplate spectrophotometer reader (Molecular Devices, USA). And the cell viability of the control group was regarded as 100%. The experiments were performed in triplicate of each flavonol.

2.1.4 Measurement of NO

RAW264.7 cells were seeded in 24-well plates at a density of 4×10^4 cells/well and incubated overnight at 37 °C with 5% CO_2. After pre-treatment with indicated concentrations of three flavonols for 4 h, cells were stimulated with LPS (1μg/ml) for another 12 h. Then, 100 μL supernatants of were transformed into a new 96-well plate. And the Griess reagent was added and the 96-well plate was shaken for 30 min in dark conditions. The absorbance of the final solution was measured at 540 nm by a microplate reader. The inhibition rates of NO release were shown to express the percentage of NO production in flavonols and only LPS groups. This assay was performed in triplicate.

2.1.5 Enzyme Linked Immune Sorbent Assay (ELISA)

RAW 264.7 cells were pretreated with different concentrations of fisetin, quercetin, and myricetin for 4 h and stimulated with LPS (1 μg/mL) for 12 h. The cell supernatant samples were collected to detect the cytokine levels of IL-6 and TNF-α by

ELISA kits according to the manufacturers' protocols. The absorbance at 450 nm was read through a microplate spectrophotometer reader.

2.1.6 Detection of intracellular ROS production

RAW 264.7 (2×10^5 cells/well) cells were seeded in 6-well plates and cultured for 12 h. Cells were pretreated with fisetin at 20 μM, quercetin at 40 μM, and myricetin at 80 μM for 4 h, and exposed to LPS (1μg/ml) for 12 h. DCFH-DA reagent (10 mM) was diluted to 5 μM by DMEM (1:2000) in dark condition. The cells were discarded and added 1 mL DCFH-DA diluted solution, incubating at 37 ℃ for 20 min. Then, the solution was discarded and cells were washed three times with DMEM to remove DCFH-DA that existing on the cell surfaces. Finally, cells were collected into 1.5 mL tubes and suspended with 200 μL PBS to determine the intracellular ROS production by flow cytometer (Beckman, USA). The FlowJo software (BD, America) was conducted for analysis.

The immunofluorescence analysis was also done to investigate the ROS production. The preliminary procedure was almost the same as for flow cytometer detection. However, the cells were not need to be collected instead of filling with 300 μL PBS, and they were taken photos using DMI8 inverted fluorescent microscope (Leica, Germany).

2.1.7 Western blot analysis

RAW 264.7 (2×10^5 cells/well) cells were seeded in 6-well plates and cultured for 12 h. Cells were stimulated with LPS (1μg/mL) for 30min or 12 h in the absence or presence of different concentrations of flavonols for 4 h. The supernatants were discarded after centrifugating for 6 min at 2000 rpm. And 100 μL RIPA buffer containing with 1% protease inhibitor cocktail and 1% phenylmethylsulfonyl fluoride (PMSF) (Beyotime, China) was added into harvested cells and incubated for 40 min on ice. Then they were centrifuged (1500 rpm, 15 min) at 4 °C and collected the supernatants to obtain the total protein. Nuclear protein was fractionated with nuclear extraction reagent from Nuclear and Cytoplasmic Protein Extraction kit (Beyotime, China) according to the manufacture's instruction. The concentrations of total protein and nuclear protein were determined by Thermo Pierce BCA protein assay kit (Thermo Scientific, USA). Proteins were dissolved by SDS/PAGE loading buffer and

boiled for 10 min at 99 °C. Subsequently, the same amounts of protein (20 μg) were isolated by 8%-10% SDS-PAGE gels and transferred to polyvinylidene fluoride (PVDF) membranes (Bio-Rad, USA). The membranes were blocked by 5% de-fatted dry milk in Tris-Buffered Saline/Tween 20 (TBST) for 1 h and probed with corresponding specific primary antibodies diluted with TBST at 1:1000 overnight at 4 °C (GAPDH, Lamin B, IκBα, p-IκBα, NFκB p65, p-p65, JNK, p- JNK, ERK, p-ERK, MEK, p-MEK, and iNOS). The membranes were washed with TBST for 3 times and incubated with the secondary antibody diluted with TBST at 1:2000 for 1 h at room temperature. After washing with TBST for another 3 times, the protein bands were visualized by an enhanced chemiluminescence detection kit and scanned by Bio-Rad ChemiDoc™ MP Imaging System (Bio-Rad, USA). The bands were quantified by Image J densitometry software.

2.1.8 Immunofluorescence assay

RAW 264.7 cells (1×10^4) were cultured in the confocal dishes (NEST Biotechnology Co., Ltd, China) overnight. Then, cells were pretreated with the highest concentration of selected flavonols for 4 h, followed by inducing LPS (1 μg/ mL) for 30 min. After treatment and stimulation, cells were washed with cold PBS for 3 times and immediately fixed in 4% paraformaldehyde for 15 min. Cold PBS was used to washed the cells for another three times and 0.5% Triton X-100 solution was added for cell permeabilization for 20 min at room temperature. Next, cells were blocked with 3% BSA for 1 h in the cell incubator and followed by incubating with primary antibody rabbit NF-κB p65 (1: 500 dilution) for 2 h at room temperature. Cells were washed with ice-cold PBS for 3 times and incubated with secondary antibody Alexa Fluor 568 goat anti-rabbit IgG (H+L) (1:500 dilution) for 1 h at dark at room temperature. Lastly, cells were stained by 4',6-diamidino-2-phenylindole (DAPI) for 10 min at dark for labeling cell nucleus and photographed by Leica TCS SP8 Confocal Laser Scanning Microscope System (Leica, USA).

2.1.9 Metabolism of flavonols in RAW264.7 cells

RAW cells were cultured in 6-well plates of DMEM (10% FBS) culture medium without P/S. Different time points (5 min, 30 min, 6 h, 16h) after adding flavonols were set up to collect the cells. The concentration treatments of flavonols and LPS

were the same as 2.3. Besides, LPS did not added into cells at 5 min and 30 min, but added after pretreating flavonols for 4 h. At different time points, 500 μL of cell culture medium supernatant was removed and pipetted into a 1.5 mL centrifuge tube containing 1,000 μL of methanol (HPLC grade, -20 ^{o}C). The remaining medium was immediately discarded and cells were washed with 1 mL PBS three times. Cells were then scraped using 100 μL MiliQ water once and 100 μL of methanol (HPLC grade, -20 ^{o}C) twice respectively. The solutions were combined in a 1.5 mL centrifuge tube and sonicated at 0^{o}C for 30 min. Finally, all tubes were centrifuged at 20,627 ´ g for 15 min at 0 ^{o}C and the supernatants were used to analyse the metabolism of flavonols in RAW264.7 cells by UPLC- LTQ Orbitrap XL hybrid FTMS system in positive ion (ESI) mode. All the experimental conditions were same as described in 2.4 at positive ion (ESI) mode.

UPLC-MS/MS analysis was performed on a Thermo UltiMate 3000 UHPLC system and a Thermo Scientific LTQ Orbitrap XL hybrid FT Mass Spectrometer (San Jose, CA, USA). Chromatographic separation on the system was achieved on a Waters ACQUITY UPLC HSS T3 1.8 μm, 2.1 × 150 mm column (Waters Technology, USA). The mobile phase was a gradient of 0.1% formic acid in MiliQ water (A) and acetonitrile (B) at a flow rate of 0.3 mL/ min. The injection volume was set at 10.0 μL. The elution gradient was set as follows: 0-5 min, 15% B; 5-10 min, 15-25% B; 10-20 min, 25-40% B; 20-25 min, 40-45% B; 25-30 min, 45-15% B. The MS detection was carried out by using electrospray ionization (ESI) on positive ionization mode with capillary temperature of 380^{o}C, sheath gas (N_2) flow rate of 48 arbitrary units (arb), auxiliary gas flow rate of 15 arb and ion spray voltage of 4.5 kV. The acquisition time was 30 min and full MS scans were acquired in the range of m/z 80-1500 with a mass resolution of 30,000. MS^1 and MS^2 data including retention time, quasi-molecular ions and fragment ions information were collected using Xcalibur software (Thermo Fisher Scientific, CA, USA) for data collection and analysis. These data were combined with the characteristic fragment ions, chemical structure and reaction characteristics of fisetin, quercetin, and myricetin to analyze the cell metabolism of RAW cells.

2.1.10 Statistical analysis

All data were analyzed by GraphPad Prism 7 software and shown as mean ± SD. Significant differences between the experimental groups were determined through

one-way ANOVA. $p < 0.05$ was regarded statistically significant. Every experiment was conducted for at least three times.

2.2 Results

2.2.1 Toxicity of flavonols on RAW 264.7 cells

In order to evaluate whether flavonols (Fis, Que, and Myr) have potential cytotoxicities at their texted concentrations (**Fig. 2.1A**), MTT assay was used to determine the cell viabilities of flavonols on RAW 246.7 cells. Cells were incubated with flavonols for 24 h and results showed that the safe concentrations of flavonols were Fis at 5, 10, and 20 μM, Que at 10, 20, and 40 μM, and Myr at 20, 40, 80 μM (**Fig. 2.1B**). Therefore, these selected concentrations were non-toxic and could be used in the following experiments *in vitro*.

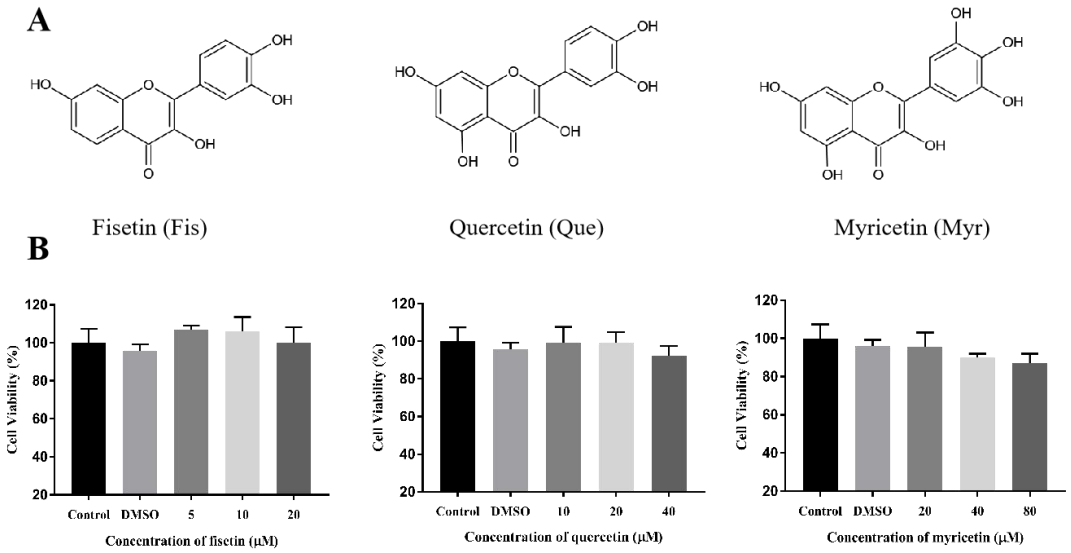

Fig. 2.1. Toxicity of flavonols on RAW 264.7 macrophages. (A) The chemical structures of flavonols were drawn by KingDraw software. (B) Cells were pretreated with different concentrations of flavonols for 24 h and detected by MTT assay. Data were expressed as mean ± SD.

2.2.2 Flavonols inhibited LPS-induced NO release and pro-inflammatory proteins production in RAW264.7 cells

The inhibition effects of inflammatory responses were evaluated and compared

among fisetin, quercetin, and myricetin. Excessive NO production is a typical sign of inflammation in activated RAW264.7 cells (Wu et al., 2018). All three flavonols could dramatically inhibited NO release dose-dependently under the Dunnett's multiple comparisons test (**Fig. 2.2A**). Specifically, the inhibitory rates of NO production were 6.84%, 17.92%, and 51.92% in Fis group of 5, 10, and 20 μM, 20.25%, 36.67%, and 59.97% in Que group of 10, 20, and 40 μM, and 14.47%, 17.71%, and 25.91% in Myr group of 20, 40, 80 μM. Regarding the same concentration of 20 μM for comparison, fisetin has the strongest inhibition effect (51.92%) of NO release, and quercetin ranked second. However, myricetin showed the least inhibition effect (14.47%) at 20 μM, and it only had 25.91% inhibition rate even at its highest concentration at 80 μM. The iNOS protein played a vital role during inflammation (Fu et al., 2014). Based on the effective inhibition rate of NO, the Western blotting was performed to evaluate whether the NO release was related to the protein modulation of iNOS expression. The result showed that LPS significantly increased the expression of iNOS protein, which could be reversed by three flavonols with variable effects (**Fig. 2.2D & 2.2E**). Similarly, the expression levels of iNOS were inhibited to the greatest extent by fisetin at 20 μM, followed by quercetin, while myricetin had the lowest effect. This result was consistent with that of NO inhibition.

In addition, great amounts of pro-inflammatory proteins were produced by activating macrophages when the inflammation triggers (Su et al., 2017). LPS strongly increased the expression levels of IL-6 and TNF-α, which were reduced by flavonols in dose-dependent manners (**Fig. 2.2B & 2.2C**). Notably, these inflammatory mediators' expressions were recovered greatly by Fis group at 20 μM treatment. Taken together, the above research data implied that three flavonols effectively suppressed LPS-stimulated inflammatory responses in macrophages and among which fisetin exhibited the strongest anti-inflammatory effect.

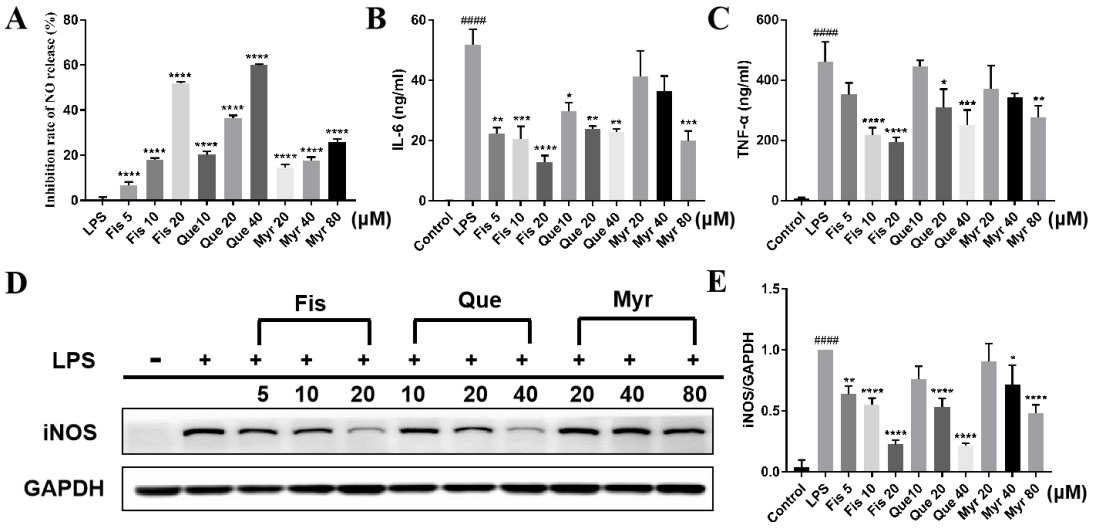

Fig. 2.2. The inhibition effects of flavonols on inflammatory responses. RAW 264.7 cells were pretreated with different concentrations of flavonols for 4 h and then induced with LPS (1 μg/ml) for 12 h. The supernatants were used for (A) detection of inhibition rate of NO release with Griess reagent and determination of (B) IL-6 and (C) TNF-α with ELISA kits. The cells were collected for analysis of (D&E) iNOS expression by western blotting. Data were mean ± SD. *$P < 0.05$, **$P < 0.01$, ***$P < 0.001$, and ****$P < 0.0001$ versus LPS, $^{\#\#\#\#}P < 0.0001$ versus Control.

2.2.3 Flavonols suppressed LPS-induced ROS production in RAW264.7 cells

It's reported that inflammation is closely related to oxidative stress, meaning for increasing intracellular ROS levels. And ROS was regarded as one of the inflammatory mediators (Ji et al., 2018). Flow cytometry analysis was performed to text the ROS levels under LPS (1 μg/mL, 12 h) induction. LPS stimulated excessive ROS production in cells compared with the control group, while the ROS productions were decreased in the presence of all selected flavonols, especially in fisetin group at 20 μM (**Fig. 2.3A & 2.3B**). Moreover, the ROS levels were also captured by Lecia DMI8 microscope, with the same tendency as flow cytometry results (**Fig. 2.3C**). These data confirmed that three flavonols had the ability to reverse LPS-induced ROS production to some extent. And fisetin could regain the ROS level closed to the control group.

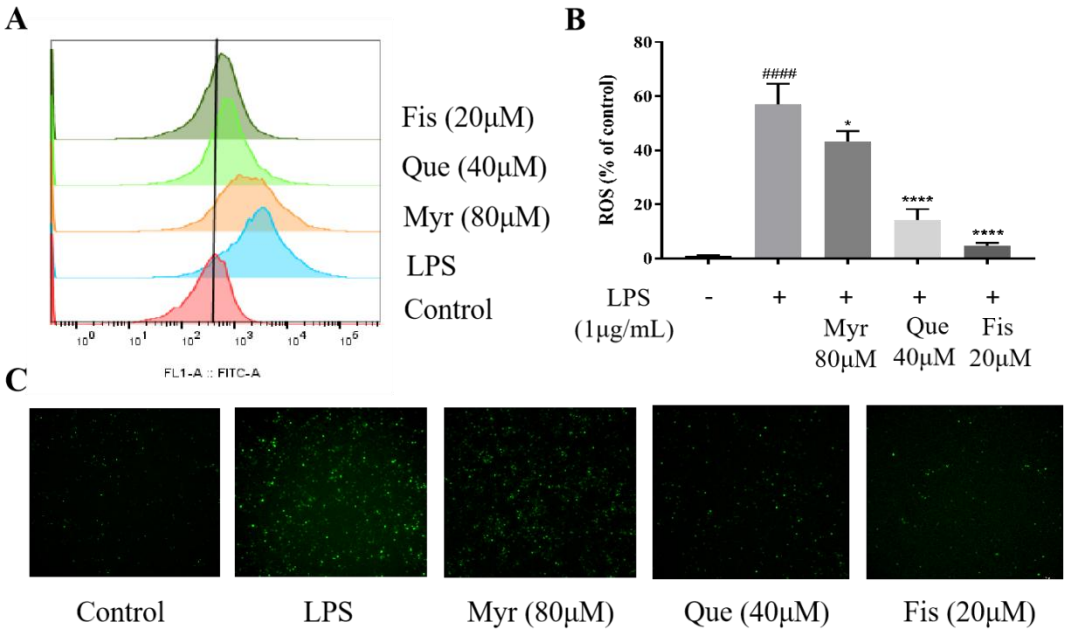

Fig. 2.3. Effects of flavonols on intracellular ROS in LPS-induced RAW264.7 cells. Cells were pretreated with flavonols for 4 h and induced with LPS (1 μg/ml) for 12 h, then they were incubated with DCFH-DA. Positive cells were (A&B) counted by cell flow cytometry and (C) visualized by Leica DMI8 fluorescence. Values were mean ± SD. **P* < 0.05 and *****P* < 0.0001 versus LPS, $^{\#\#\#\#}P$ < 0.0001 versus Control.

2.2.4 Flavonols blocked the activation of MAPK signaling pathways in LPS-induced RAW264.7 cells

To further explore whether the anti-inflammatory effects of flavonols are associated with MAPK signaling pathways, the expressions of phosphorylation of JNK, ERK, and MEK proteins were investigated by western blotting assays. RAW264.7 cells were pre-treated with flavonols and stimulated with LPS (1.0 μg/ml) for 30 min. As shown in **Fig. 2.4A**, the ratios of p-ERK/total ERK and p-MEK/total MEK were up-regulated substantially by LPS but inhibited by Fis especially at 20 μM. However, the protein expressions of p-JNK/total JNK showed slightly decrease with no significant difference between LPS group and Fis group. Regarding for Que group, the expressions of p-ERK/total ERK and p-MEK/total MEK were remarkably lower than LPS group at the concentration of quercetin 20 and 40 μM (**Fig. 2.4B**). But Que group also showed mild decrease but did not have significant difference in p-JNK/total JNK expression compared to LPS group. Notably, myricetin could down-regulated p-JNK, p-ERK, and p-MEK protein expressions apparently at 80 μM (**Fig. 2.4C**). Therefore,

the anti-inflammatory activities of fisetin, quercetin, and myricetin were partially via blocking the activation of MAPK signaling pathways.

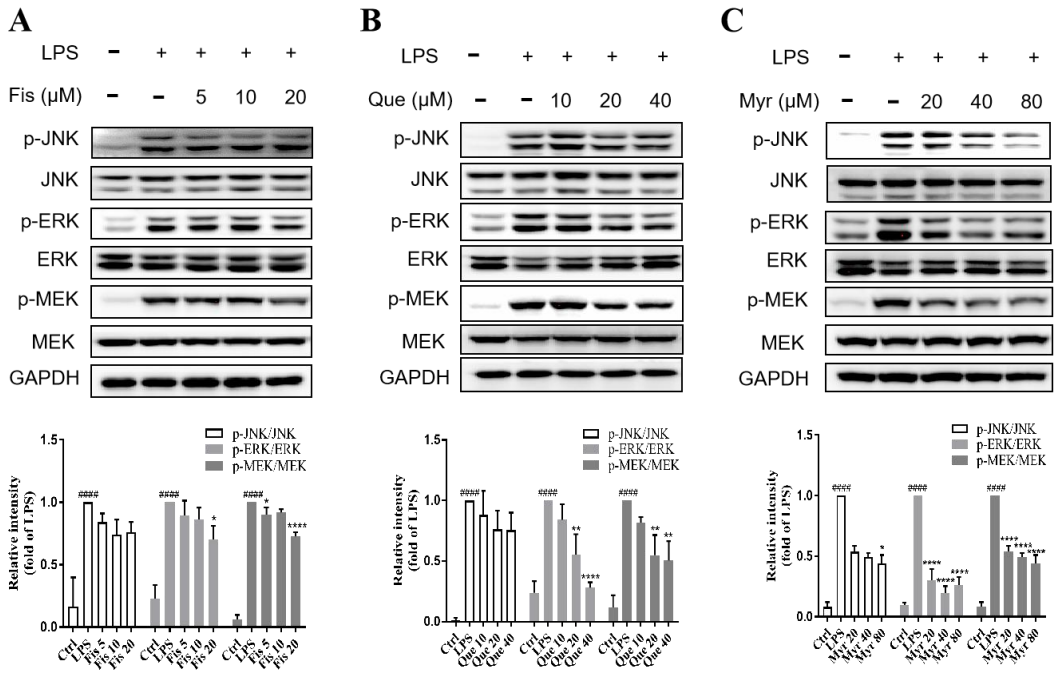

Fig. 2.4. Effects of flavonols on the activation of MAPK signaling pathways in LPS-induced RAW264.7 cells. Cells were pretreated with flavonols for 4 h and induced with LPS (1 μg/ml) for 30 min. The protein expression levels of p-JNK, JNK, p-ERK, ERK, p-MEK, and MEK in fisetin (A), quercetin (B), and myricetin (C) were determined by western blotting. Values were mean ± SD. *$P < 0.05$, **$P < 0.01$, and ****$P < 0.0001$ versus LPS, $^{\#\#\#\#}P < 0.0001$ versus Control.

2.2.5 Flavonols inhibited the activation of NF-κB signaling pathways in LPS-induced RAW264.7 cells

NF-κB is a typical transcription factor for regulating inflammatory genes expression in LPS-induced inflammation (Linghu et al., 2020). To find out the molecular mechanisms of inflammatory suppression of flavonols, the effects of NF-κB signaling pathways were investigated by western blot. The expressions of phosphorylated-p65 and IκBα proteins were increased in LPS-induced RAW264.7 cells, but they were reversed through fisetin treatment at the highest concentration at 20 μM (**Fig. 2.5A**). And these proteins were markedly declined at the middle and high dose of quercetin treatment (**Fig. 2.5B**). In addition, myricetin could decrease these proteins expressions in a dose-dependent manner (**Fig. 2.5C**). The nuclear

translocation of p65 protein is an important step for the activation of NF-κB pathway, so the nuclear cell fractions were separated for determination of subcellular compartmentalization of p65 (Tu et al., 2019). Results showed the the nuclear expression levels of NF-κB p65 were dramatically increased in the LPS stimulation compared with control group, while flavonols pretreatment blocked the LPS-induced nuclear accumulation of NF-κB p65 with variable influences. The inhibition effects were significant in Fis and Que groups at their 20 μM (**Fig. 2.5D & 2.5E**), while at 40 and 80 μM in Myr group (**Fig. 2.5F**). An immunofluorescence assay was performed to reconfirm the location of NF-κB p65 in the absence or presence of LPS and flavonols. The red color intensity which presented the p65 fluorescence was accumulated into the nucleus after LPS induction, but it was reversed by flavonols treatment, which was nearly the same intensity and shape as the control group (**Fig. 2.5G**). Overall, these data implied that three flavonols significantly blocked LPS-stimulated NF-κB signaling pathways.

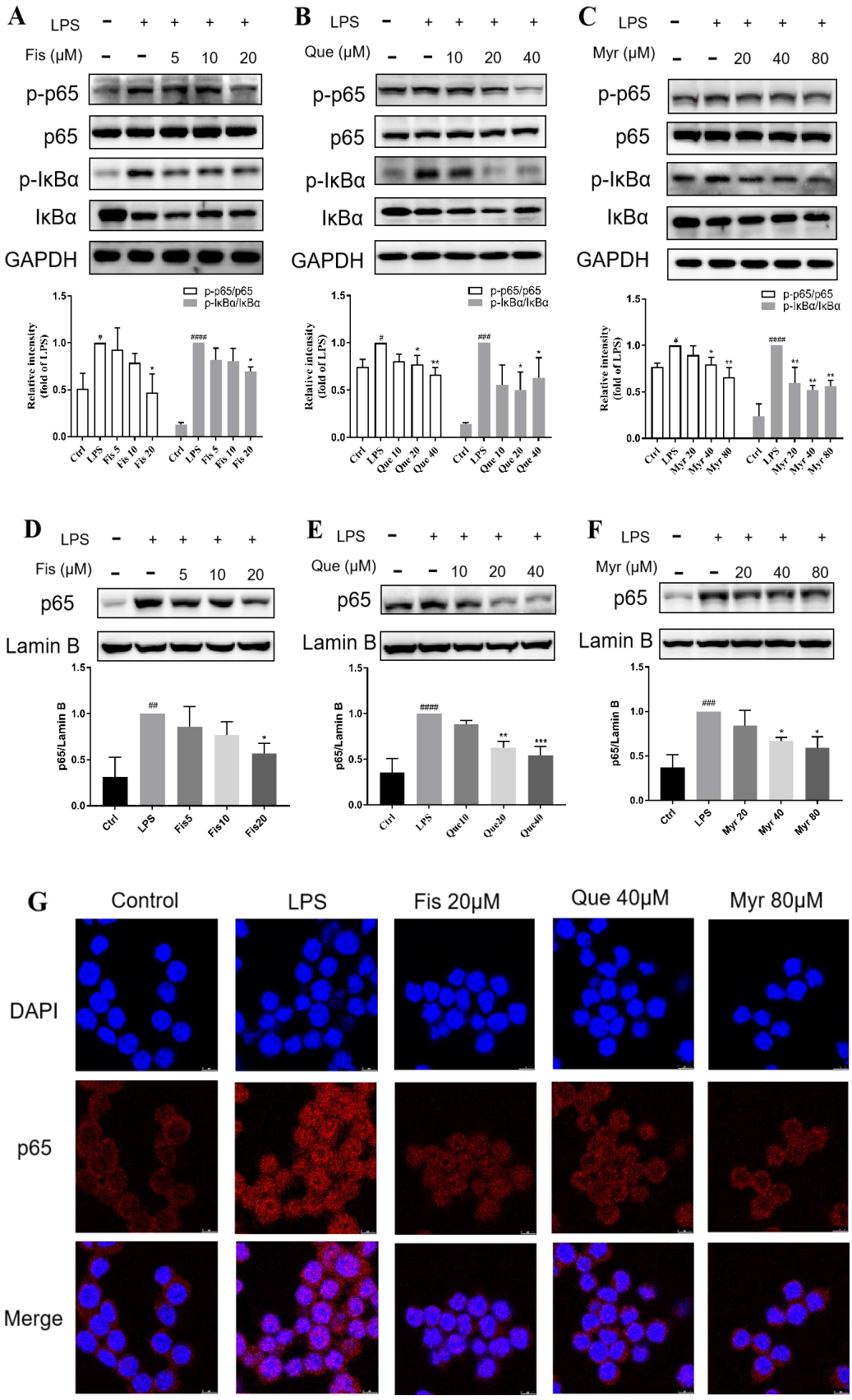

Fig. 2.5. Effects of flavonols on the activation of NF-κB signaling pathways in LPS-induced RAW264.7 cells. Cells were pretreated with flavonols for 4 h and induced with LPS (1 μg/ml) for

30 min. The protein expression levels of p-IκBα, IκBα, p-p65, and p65 were performed by western blotting from total cell lysates in fisetin (A), quercetin (B), and myricetin (C). The levels of nuclear p65 were texted in fisetin (D), quercetin (E), and myricetin (F) by western blotting. And Lamin B was regarded as internal loading controls. Immunofluorescence staining of nuclear p65 by confocal microscopy (G). Red fluorescence represented p65 protein and blue fluorescence (DAPI) indicated nuclei. Values were mean ± SD. $^{*}P < 0.05$, $^{**}P < 0.01$, and $^{***}P < 0.001$ versus LPS, $^{\#}P < 0.05$, $^{\#\#}P < 0.01$, $^{\#\#\#}P < 0.001$, and $^{\#\#\#\#}P < 0.0001$ versus Control.

2.2.6 Metabolic situation of flavonols in RAW264.7 cells

To further reveal the *in vitro* mechanisms of anti-inflammatory effect in RAW264.7 macrophages, it is necessary to explore the metabolic situation of flavonols in cells. Medium with flavonols were added into cells and collected them at different time points (5 min, 30 min, 6 h, and 16h) by UPLC-MS/MS analysis. Fisetin, quercetin, and myricetin quickly entered the cells at only 5 min and degraded at different times. As shown in **Fig. 2.6A**, the methylation reaction was speculated in fisetin in the molecular weight (Mw) of 301.07 at 5 min. The intensity of methylated fisetin was increased continuously and accumulated to the maximum value at 16 h. Glucuronidation degradation of fisetin was detected (Mw: 463.09) later. Finally, fisetin was both methylated and glucuronidated according to the Mw of 477.10. Regarding to quercetin, it degraded rapidly from 5 min to 30 min and mainly transformed into methylated quercetin at the Mw of 317.06 (**Fig. 2.6B)**. Myricetin was degraded quickly as well and then changed to methylated myricetin (Mw: 333.06). However, methylated myricetin product was almost undetectable at 30 minutes (**Fig. 2.6C**).

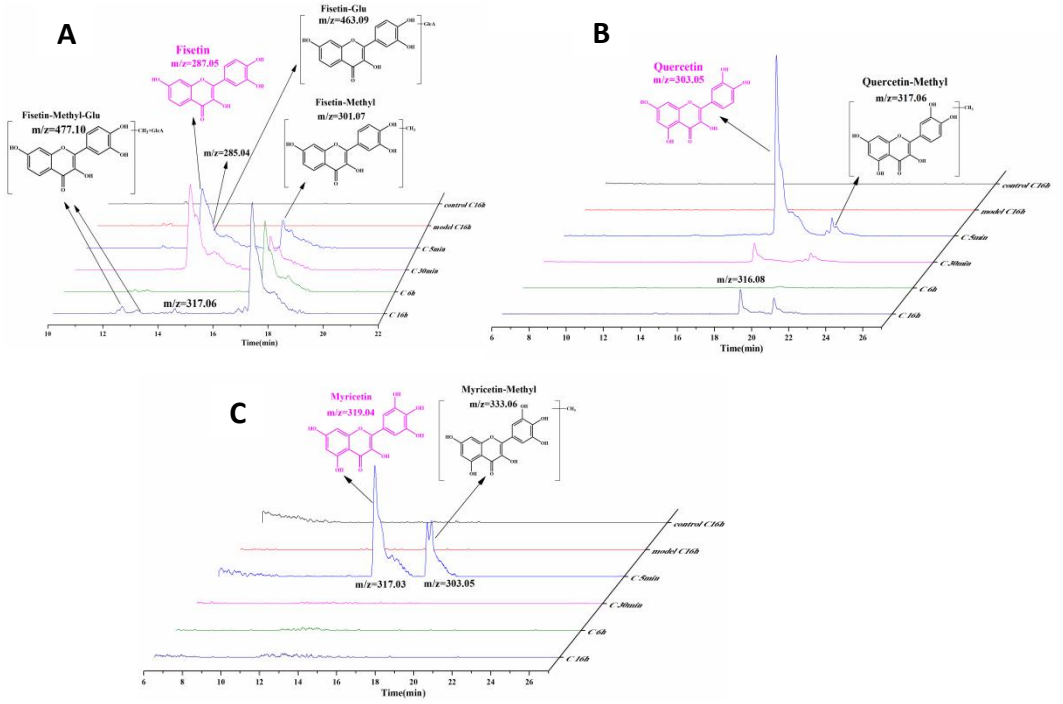

Fig. 2.6. The metabolism situation of flavonols with their degraded metabolites in RAW264.7 cells. (A) fisetin, (B) quercetin, and (C) myricetin.

2.3 Discussion

RAW 264.7 macrophages are transformed from the Abelson leukemia virus, which is an ideal model for studying inflammatory effect. And LPS can fully activate macrophages to trigger inflammation, which is mediated by NO release (Hwang et al., 2019; Malayil et al., 2020). NO is a kind of free radicals to regulate human body functions, but excessive NO synthesized by iNOS will lead to autoimmune disorders, cytotoxicity, and inflammation (Zhang et al., 2019). In the present study, the Griess assay and Western blot analysis implied that the NO overproduction was related to iNOS overexpression when LPS triggered. Flavonols suppressed the production of NO, which were highly consistent with the down-regulation of iNOS protein. In addition, fisetin treatment presented the greatest inhibition effect (**Fig. 2.2A & 2.2D-E**). Excessive NO release could stimulate proinflammatory cytokines and these cytokines mediators could promote the NO production simultaneously, which formed a positive feedback loop leading to increased inflammation (Zhang et al., 2020). All selected flavonols markedly inhibited the proinflammatory cytokines of IL-6 and TNF-α (**Fig. 2.2B & 2.2C**).

Oxidative stress played a critical role in inflammatory diseases, of which ROS level was an important mediator. Excessive ROS production disrupted the balance of oxidant/antioxidant in the human bodies, leading damages to lipids, protein, and DNA (Wang et al., 2021). DCFH-DA cell-permeable fluorescent probe is commonly used to determine intracellular ROS levels in cells or tissues by flow cytometry or confocal microscopy (Shen et al., 2018). The flow cytometry and fluorescence images showed that flavonols especially fisetin dramatically decreased the ROS generations in LPS-induced macrophages, indicating flavonols could prevent RAW264.7 cells from oxidative stress by inflammation (**Fig. 2.3**).

MAPKs and NF-κB signaling pathways are activated through LPS stimulation to regulate pro-inflammatory molecules. MAPKs belong to serine-threonine protein kinases which can regulate many cellular activities such as cell inflammatory responses via modulating pro-inflammatory molecules (Chen et al., 2017). The main components of JNK, ERK, and MEK with their phosphorylation forms from MAPK signaling pathways were examined in this research. Flavonols significantly blocked JNK, ERK, and MEK phosphorylation in LPS-induced RAW264.7 cells (**Fig. 2.4**), which implied that the inhibition effect of MAPK may be involved in suppressing anti-inflammatory effect by flavonols. The transcriptional factor NF-κB has been proved to be an up-stream signal in inflammatory cascade reaction which can increase the chemokines and pro-inflammatory cytokines expressions including IL-6, TNF-α, iNOS, *etc* (Liu and Malik, 2006; Park et al., 2007). NF-κB exists in an inactive form in resting cells which is bound with IκB-α protein in the cytoplasm. However, the IκB-α would activate and degradated upon LPS stimulation, then NF-κB would translocate into the nucleus and finally promote variable pro-inflammatory genes (Gilroy et al., 2004; Pham et al., 2017). Therefore, the effects of flavonols on NF-κB were examined. The result presented that flavonols remarkably attenuated the phosphorylation of IκB-α and p65 and blocked the accumulation of NF-κB p65 to nucleus (**Fig. 2.5**). It has been demonstrated that MAPKs modulated NF-κB pathway. Inhibiting MAPK pathway could suppress the NF-κB activation (Surh et al., 2001; Zhong et al., 2012). To sum up, the suppression of inflammatory cytokines and mediators of three flavonols were probably via blocking MAPK and NF-κB signaling pathways. And the suppression of NF-κB might be at least partially attributed to the inhibition of MAPK.

Moreover, the metabolic situation of flavonols in RAW264.7 cells was explored.

Several degradation products of fisetin were formed by methylation and glucuronidation. And quercetin and myricetin were transformed into several new products, including methylated quercetin and methylated myricetin, respectively (**Fig.6**). All flavonols were entered the cells quickly and transformed into many forms of metabolites, indicating many metabolites were took functions in cells, which were closely associated with the pharmacological activities. Further studies should focus on the relationship between the exact metabolites and the bioactivities.

2.4 Brief conclusion

This research proved the flavonols of fisetin, quercetin, and myricetin exerted anti-inflammatory effects in LPS-induced RAW 264.7 cells. Fisetin, quercectin, and myricetin can inhibit NO and ROS production in LPS-stimulated RAW264.7 cells. These flavonols reduced the expression levels of ROS, TNF-α, and IL-6 and suppressed the activation of NF-κB and MAPK pathways by partially reducing the levels of phosphorylation of IκBα, p65, JNK, ERK, MEK, and the nuclear translocation of NF-κB p65 **(Fig. 2.7)**. Fisetin is an excellent anti-inflammatory reagent which can be treated as potential adjuvant treatment for inflammation. The structure-activity relationship among flavonols and the *in vivo* experiments should be explored in the future.

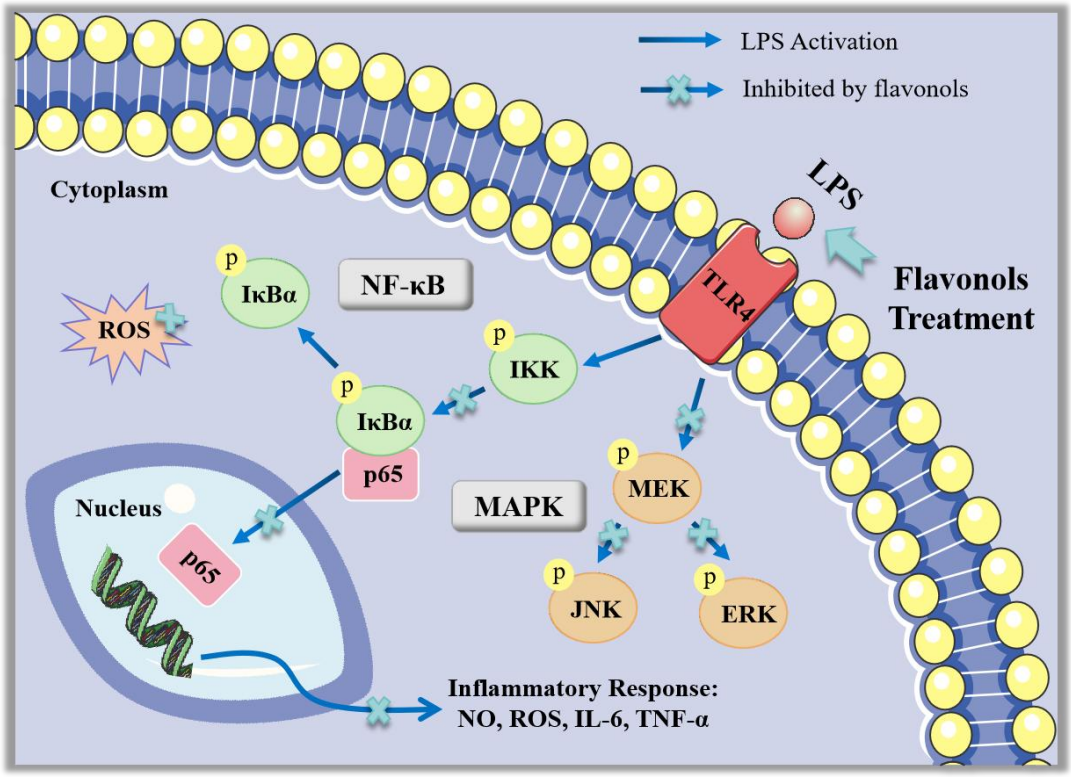

Fig. 2.7. The molecular mechanism of flavonols against LPS-induced inflammation.

Chapter 3 Fisetin ameliorates D-GalN/LPS-induced acute liver injury by inhibiting inflammation in C57BL/6 mice

3.1 Materials and Methods

3.1.1 Chemicals and reagents

Lipopolysaccharide (Escherichia coli, O55: B5) and Silymarin were purchased from Sigma (St. Louis, MO, USA). D-galactosamine (D-GalN) was obtained from aladdin (Shanghai, China). Fisetin was purchased from Tokyo Chemical Industry Co., Ltd. Aspartate aminotransferase (AST) and alanine aminotransferase (ALT) biochemical assay kit were commercially obtained from Nanjing Jiancheng Bioengineering Institute (Nanjing, China). TNF-α, IL-6, IL-1β were obtained from Jiangsu Meimian industrial Co., Ltd. Catalase (CAT) and Malondialdehyde (MDA) were purchased from Solarbio (Beijing, China). Primary antibodies against IκBα, NFκB p65, phosphorylated (p)-IκBα, p-p65, GAPDH and the secondary antibody were acquired from Cell Signaling Technology (Danvers, MA, United States).

3.1.2 Animal treatment and experiment design

Male C57BL/6 mice (6-8 weeks old, weighing 19-21g) were purchased from Zhuhai BesTest Bio-Tech Co,.Ltd. (Zhuhai, China). They were housed under specific-pathogen-free (SPF) conditions at the temperature of 20 ± 3 °C and humidity of 55 ± 10% with 12 h light/dark cycle. In the acclimatization period, all mice were given free access to water and normal diet. The animal experiment was in accordance with daily laboratory animal welfare guidelines and approved by committee of laboratory animal ethics of Guangdong Ocean University (GDOU-LAE-2021-015).

Mice were randomly separated into Control group, Model group, Fisetin group, and Silymarin group as positive drug with nine mice in each group. After adaptive feeding, Control group and Model group were daily orally administrated with 0.3% CMC-Na. Fisetin group and Silymarin group were given fisetin (100mg/kg, suspended in 0.3% CMC-Na) and Silymarin (100mg/kg, suspended in 0.3% CMC-Na) for 4 weeks.

Except for the Control group, other mice were intraperitoneally injected with D-GalN (500 mg/kg) and LPS (50 μg/kg) to established acute liver injury after the last administration. The mixture of D-GalN and LPS were dissolved in PBS. Mice were sacrificed after 4 h of stimulation. Blood samples and liver tissues were collected and snap frozen in liquid nitrogen. Then they were removed quickly to store at -80˚C. The liver tissues were fixed at 4 % paraformaldehyde.

3.1.3 Body weight and liver index

During 4 weeks of the administration, the body weight of each mouse was detected on the day 0, 7, 14, 21, and 28. The weight change in every group were gained by calculating the weight of day 28 minus day 0. The liver index was noted by liver weight dividing by body weight at the time of sacrifice.

3.1.4 Serum biochemical assays

The Hepatic functions of AST and ALT were evaluated in plasma with commercial kits. Inflammation cytokines of IL-1β, IL-6, TNF-α were detected following the manufacturers' instructions.

3.1.5 Liver homogenate biochemical assays

The oxidative stress of liver tissue such as MDA and CAT were analyzed by commercial kits.

3.1.6 Liver histopathology

A portion of liver tissues in different groups were fixed in 4 % paraformaldehyde and then stained with hematoxylin-eosin (H & E) to observe the histopathological changes based on previous report (Khan et al., 2021). The hepatic lesions were evaluated according to hepatic inflammatory cell infiltration and necrosis. Images were observed at 200 X.

3.1.7 Western blot analysis

Total proteins of mice liver tissues were dissected and homogenized using RIPA lysis buffer. The supernatants were collected after centrifuging at 13000 rpm for 15

min at 4°C. The concentrations of total protein were determined by Thermo Pierce BCA protein assay kit (Thermo Scientific, USA). Proteins were dissolved by SDS/PAGE loading buffer and boiled for 10 min at 99 °C. Subsequently, the same amounts of protein (20 μg) were isolated by 8%-10% SDS-PAGE gels and transferred to polyvinylidene fluoride (PVDF) membranes (Bio-Rad, USA). The membranes were blocked by 5% de-fatted dry milk in Tris-Buffered Saline/Tween 20 (TBST) for 1 h and probed with corresponding specific primary antibodies diluted with TBST at 1:1000 overnight at 4 °C (GAPDH, IκBα, NFκB p65, and p-p65). The membranes were washed with TBST for 3 times and incubated with the secondary antibody diluted with TBST at 1:2000 for 1 h at room temperature. After washing with TBST for another 3 times, the protein bands were visualized by an enhanced chemiluminescence detection kit and scanned by Bio-Rad ChemiDoc™ MP Imaging System (Bio-Rad, USA). The bands were quantified by Image J densitometry software.

3.1.8 Statistical analysis

All data were analyzed by GraphPad Prism 7 software and shown as mean ± SEM. Significant differences between the experimental groups were determined through one-way ANOVA. $p < 0.05$ was regarded statistically significant. Every experiment was conducted for at least three times.

3.2 Results

3.2.1 Body weight and liver index

To explore the protective function of fisetin on D-GalN/LPS-stimulated acute liver injury, mice were orally administered fisetin (100 mg/kg) and Silymarin (100 mg/kg) once of each day for four weeks before stimulation. Silymarin was regarded as the positive drug. These two compounds did not have abnormal influence on the bodyweight of mice compare with the control group, which were statistically non-significant ($p > 0.05$) (**Fig. 3.1A & 3.1B**). The liver index was higher in model group compared with control group, which were significantly reversed by the fisetin and silymarin groups (**Fig. 3.1C**).

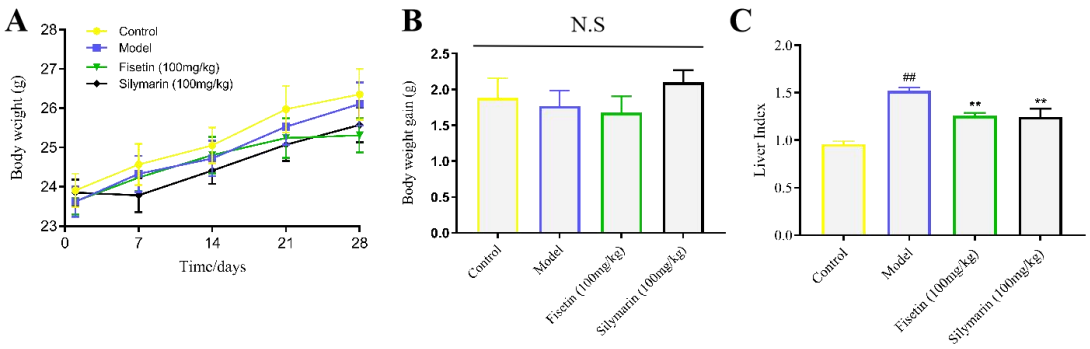

Fig. 3.1. Influence of fisetin pretreatment on body weight and liver index in different groups of mice. Body weight changes in each 7 days (A), body weight gain (B), and liver index (C). Values were mean ± SEM. $^{\#\#}P < 0.01$ versus Control, $^{**}P < 0.01$ versus Model.

3.2.2 Fisetin ameliorated D-GalN/LPS-stimulated liver pathology

The histopathology was performed to evaluate the effect of fisetin on hepatic injury. Macroscopic view showed that the liver section from untreated mice revealed normal reddish color and no obvious edema lesions. By contrast, D-GalN combined with LPS evidently caused hepatic congestion in the model group. The livers in model group became blackish with spotty haemorrhageappearances and had remarkable pathologic changes such as morphological disruption and confluent haemorrhage. However, both fisetin and silymarin treatment could decrease the hepatic congestion to some extent (**Fig. 3.2A**).

Then, H&E staining liver sections from control group showed that the hepatocytes did not have inflammatory response because of prominent nucleus and well-preserved cytoplasm with aligned in cords. Severe necrosis and massive inflammatory cell infiltration were widely seen after D-GalN and LPS stimulation in the model group compared with the control group. However, these pathological symptoms were alleviated in the pretreatment of fisetin and silymarin. The results implied that fisetin could have a protective effect on acute liver injury in mice (**Fig. 3.2B**).

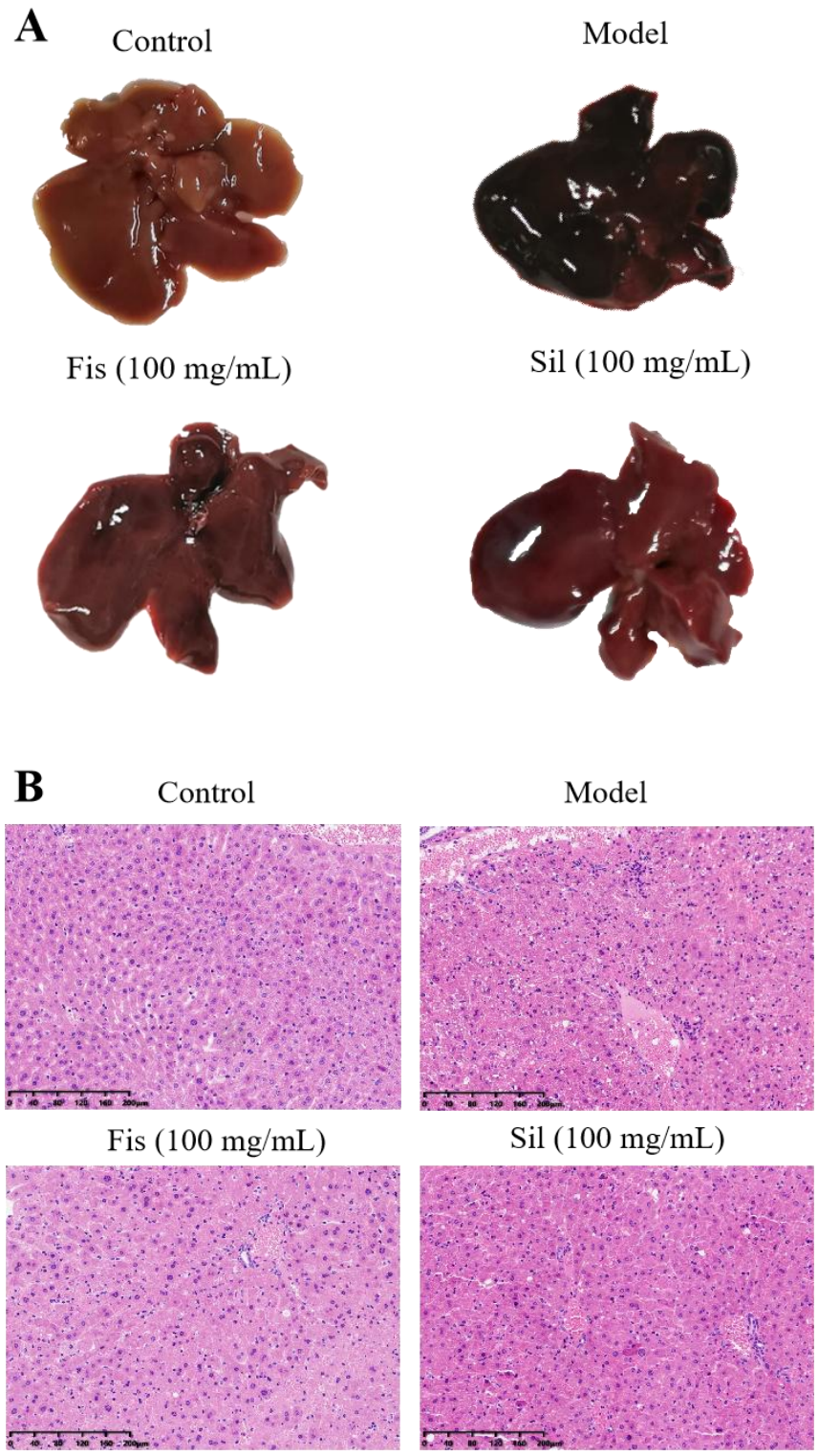

Fig. 3.2. Histopathological evaluation in different groups on ALI. Liver tissues were collected for macroscopic view (A) and stained with H&E (B).

3.2.3 Fisetin suppressed biochemical markers of acute liver injury

ALT and AST are widely considered as the informative biochemical markers for diagnosing hepatic injury and necrosis (Guo et al., 2021). D-GalN and LPS treated group witnessed sharp increases in serum AST and ALT levels ($p < 0.01$) when compared with control group. But the silymarin treatment could significantly decline the serum AST and ALT levels compared with model group. It's noteworthy that fisetin decreased the serum AST and ALT to the similar level as the silymarin treatment (**Fig. 3.3A & 3.3B**).

3.2.4 Fisetin relieved oxidative stress of acute liver injury

The endogenous antioxidants MDA and CAT levels in liver tissues from different groups were determined. Fisetin treatment declined the hepatic MDA level markedly comparing to acute liver injury model group. Although fisetin showed no significant effect on increasing hepatic CAT levels, it had upward trend compared with the model group (**Fig. 3.3C & 3.3D**).

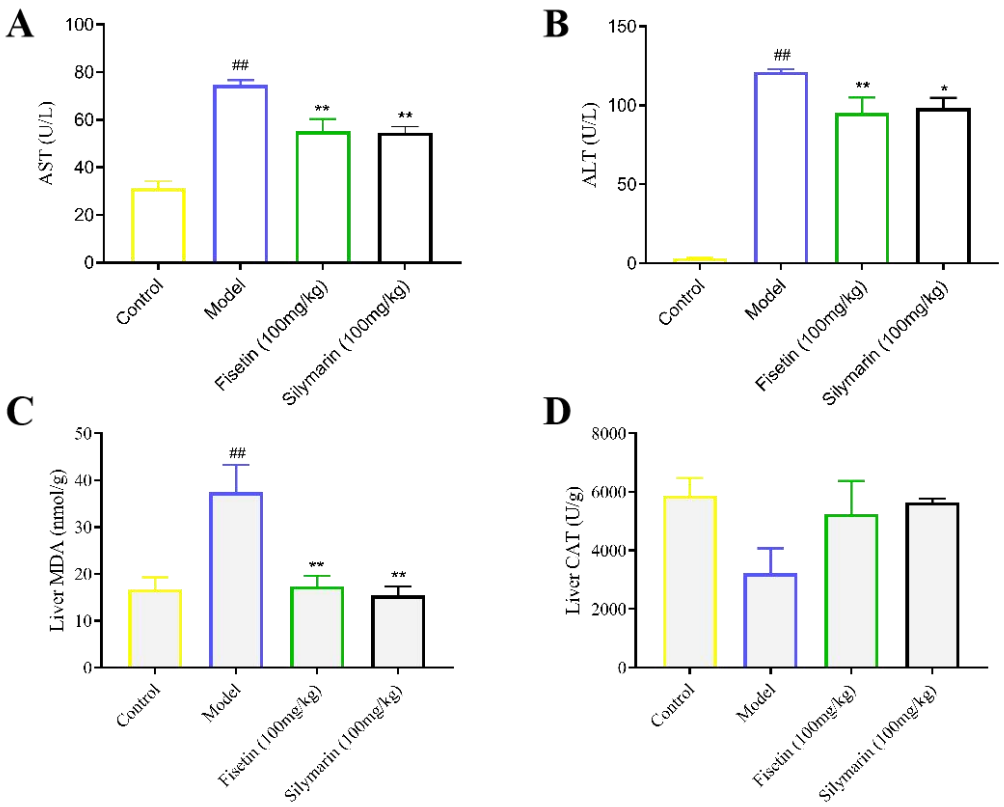

Fig. 3.3. Effect of fisetin on serum AST (A), serum ALT (B), hepatic MDA (C), and hepatic CAT (D) levels in D-GalN/LPS-stimulated liver injury. Values were mean ± SEM. $^{\#\#}P < 0.01$ versus Control, $^{*}P < 0.05$ and $^{**}P < 0.01$ versus Model.

3.2.5 Fisetin suppressed inflammatory responses of acute liver injury

The dysregulated inflammatory reaction is an important mechanism in the development of ALI by D-GalN/LPS stimulation. As shown in **Fig.3.4**, D-GalN/LPS evoked inflammation storm by dramatically increasing pro-inflammatory cytokines IL-1β, IL-6, and TNF-α. Treatment with fisetin significantly inhibited IL-1β (**Fig. 3.4A**) and IL-6 (**Fig. 3.4B**) levels, but slightly decreased TNF-α (**Fig. 3.4C**) levels in serum in comparison with model group. Regarding for the level of IL-6, positive drug silymarin group did not show excellent effect compared with fisetin treatment group. And silymarin group also slightly declined the TNF-α levels in serum. These results demonstrated that fisetin alleviated liver inflammation in D-GalN/LPS -induced acute liver injury.

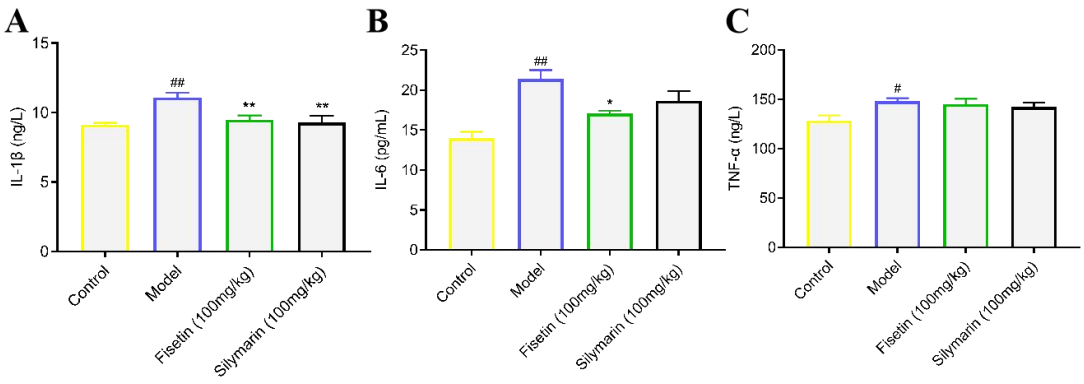

Fig. 3.4. Effect of fisetin on serum pro-inflammatory cytokines IL-1β (A), IL-6 (B), and TNF-α (C) in D-GalN/LPS-stimulated liver injury. Values were mean ± SEM. $^{\#\#}P < 0.05$, $^{\#\#}P < 0.01$ versus Control, $^{*}P < 0.05$ and $^{**}P < 0.01$ versus Model.

3.2.6 Fisetin inhibited NF-κB signaling pathway of acute liver injury

The activation of signaling pathway was explored through western blotting analysis to determine the anti-inflammatory mechanism of fisetin on ALI. The p65 protein was dramatically phosphorylated to p-p65 in ALI symptom of model group compared with the control group, whereas fisetin pretreatment could effectively inhibit the phosphorylation level of p65 ($p < 0.05$) (**Fig. 3.5A & 3.5B**). Furthermore, the IκBα protein expression of liver tissue was significantly degraded in model group when compared with control group, which could be slightly reversed by fisetin pretreatment and significantly increased by silymarin administration (**Fig. 3.5A & 3.5C**).

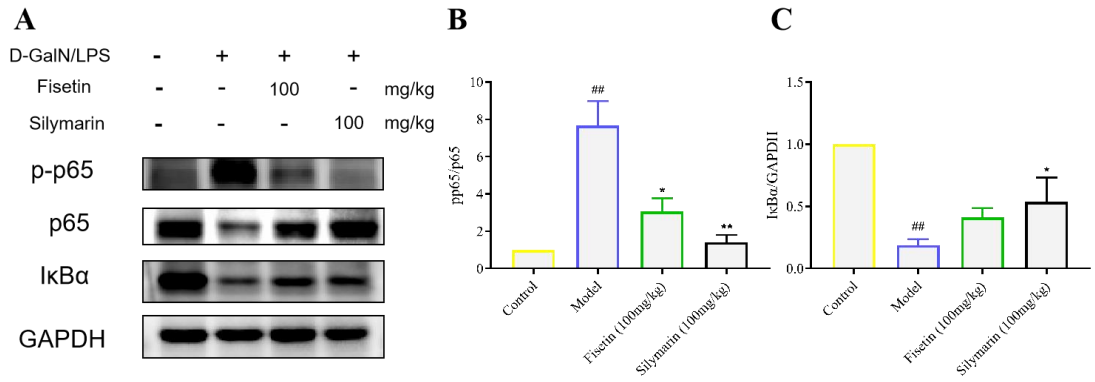

Fig. 3.5. Effect of fisetin on the activation of NF-κB signaling pathway p-p65, p65, and IκBα proteins in D-GalN/LPS-stimulated liver injury. Values were mean ± SEM. $^{\#\#}P < 0.01$ versus Control, $^{*}P < 0.05$ and $^{**}P < 0.01$ versus Model.

3.3 Discussion

Acute liver injury is a severe liver function disorder, which is manifested in hepatic encephalopathy, ascites, coagulation disorder and so on, leading to high mortality (Wang et al., 2019). Despite current efforts, the medical therapies are limited for treating ALI because its specific pathogenesis remains obscure. Liver transplantation is now the widely used therapy for patient of ALI. Suppressing inflammatory responses might be an effective approach to prevent and treat ALI (Wang et al., 2021). Anti-inflammatory agents from natural products are considered as a promising research orientation since they have fewer side effects than other agents. D-GalN combined with LPS simulated clinical liver failure, which can cause severe liver damage with hepatocyte necrosis (Hishinuma et al., 1990). Previous researches reported that fisetin exhibited strong anti-inflammatory capacity in various disease models such as kidney inflammation (Ren et al., 2020), nephropathy inflammation (Yang et al., 2019), acute pancreatitis (Jo et al., 2014), etc. Their underlying molecular mechanisms were summarized in **Fig 3.6** (Zhong et al., 2022). In this research, pretreatment of fisetin was demonstrated to ameliorate acute liver injury induced by D-GalN/LPS in mice by significantly alleviating inflammatory responses.

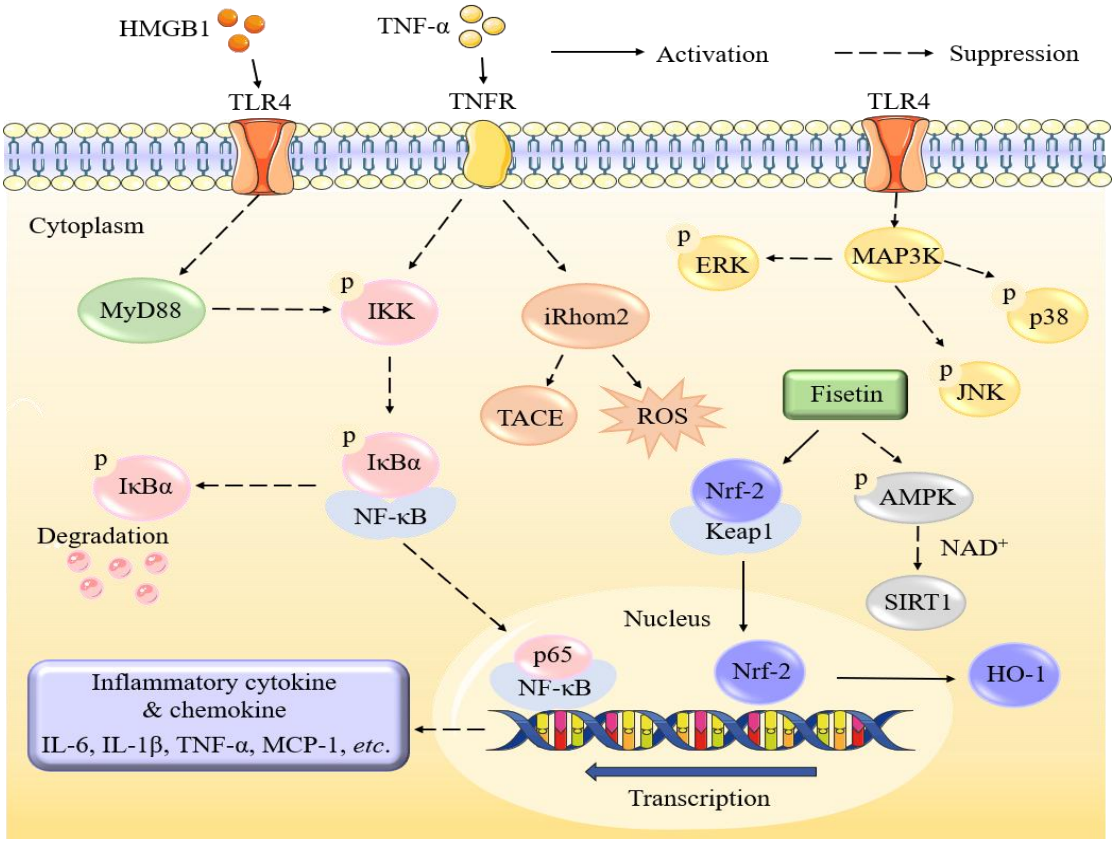

Fig. 3.6. Molecular targets of fisetin to mediate for its anti-inflammatory effect.

Biochemical markers AST and ALT together with liver index are regarded as main parameters to evaluate the severity of ALI (Bai et al., 2017). Hepatocyte damage results in the release of large amounts of hepatic AST and ALT into the bloodstream (Feng et al., 2021). Thus, the serum AST and ALT were detected in this study. The results demonstrated that D-GalN/LPS caused sharp increases in AST level, ALT level and liver index. These symptoms were consistent with the macroscopic view and H & E staining with massive neutrophils recruitment and hepatocyte necrosis when compared with control group. However, the fisetin pretreatment could evidently improve ALI symptoms by declining AST level, ALT level and liver index (**Fig3.1C, Fig 3.3A-B**). Also, liver tissue damages were alleviated through histopathological alterations compared with model group (**Fig 3.2**). These finding showed that fisetin might be an effective agent for treating D-GalN/LPS-caused ALI and inflammation.

Excessive oxidative stress promotes apoptosis and inflammation, leading to severe liver function damage (Wang et al., 2018). The anti-inflammatory activity of fisetin is often associated with free radical scavenging and antioxidant properties, with

oxidative stress elevated in high fat diet-induced nephropathy mice via inhibiting Nrf-2/HO-1 and simulating NF-κB, while they were both remarkably reversed by fisetin especially at 80 mg/kg (Chenxu et al., 2021). MDA can reflect cellular injury situation because it is a secondary metabolite produced by free-radical attack (Pan et al., 2015). CAT is regarded as antioxidant factors which suppress peroxides through catalyzing hydrogen peroxide to oxygen and water (Yao et al., 2005). In this study, intraperitoneal injection of D-GalN/LPS elevated liver MDA and suppressed CAT levels, indicating the damage of the nuclear structure and cell membrane. However, fisetin pretreatment (100mg/kg) significantly inhibited the MDA levels and slight elevated CAT activity compared with the model group (**Fig 3.3C &3D**).

The overproductions of proinflammatory cytokines (IL-6, IL-8, IL-18, IL-1β, TNF-α, and PEG2) are treated as the common vital pathogenic factors in inflammation diseases (Zhong et al., 2022). One research has shown that fisetin had anti-inflammatory effects for airway inflammation therapy in IL-1β-induced A549 cells. It effectively suppressed the expression of various chemokines (e.g. CCL5, MCP-1 and MUC5AC), inflammatory cytokines (e.g. IL-6, TNF-α, IL-8 and IL-17F), and ICAM-1 *via* inhibiting NF-κB and ERK1/2 signaling pathways (Peng et al., 2018). For acute liver injury, we found that D-GalN/LPS stimulates excessive secretion of IL-1β, IL-6, and TNF-α. Proinflammatory cytokine IL-1β is closely associated with acute liver damage because it is mainly produced by activated macrophages (Smirnova et al., 2002). Overproduction of IL-6 would trigger local or systemic inflammation by altering the insulin sensibility and insulin absorption (Guo et al., 2021). In addition, TNF-α is related to many types of inflammatory diseases and its secretion is controlled by IL-1β (Chen et al., 2020). Our results presented that the fisetin pretreatment effectively decreased serum IL-6 and IL-1β levels and slightly reduced serum TNF-α level, indicating the effectiveness of fisetin on the treatment of ALI (**Fig. 3.4**).

The activation of NF-κB signaling pathway is considered as a main contributor of inflammatory response in ALI. In resting state, NF-κB p65 combines with inhibitor protein IκBα in cytoplasm (Cutolo et al., 2013). When cell or animal models are stimulated by some signals such as LPS and TNF-α, IκBα will be degraded and separated apart from p65, promoting the cytokines releases. Subsequently, releaseing

cytokines will in turn stimulate NF-KB to form a positive feedback regulation in inflammation diseases (Wu et al., 2019). In this experiment, the protein p65 was largely phosphorylated and the IκBα was significantly degraded in the model group. However, fisetin dramatically inhibited the protein expression of p-p65 and avoided degraded IκBα protein in ALI disease (**Fig. 3.5**), suggesting that fisetin protected against ALI possibly through suppressing NF-κB signaling.

3.4 Brief conclusion

The present research clarified that the pretreatment of fisetin could alleviated D-GalN/LPS-induced ALI via reducing proinflammatory cytokines and oxidative stress in C57BL/6 mice. The underlying mechanism possibly involved NF-κB signaling pathway. Fisetin might be a promising anti-inflammatory agent to ameliorate acute liver damage.

Chapter 4 Conclusions and outlooks

4.1 Conclusions

In this study, the anti-inflammatory activities and the underlying mechanisms of fisetin, quercetin, and myricetin were investigated *in vitro*. All three flavanols exhibited anti-inflammatory effects in LPS-induced RAW 264.7 cells by inhibiting NO release, ROS production, inflammatory cytokines TNF-α and IL-6 secretion. The molecular mechanisms involved in partially suppressing the activation of NF-κB and MAPK pathways. The cell experiment found that fisetin is an excellent anti-inflammatory reagent compared with quercetin and myricetin. Therefore, we chose fisetin as the potential anti-inflammatory agent for treating D-GalN/LPS-induced acute liver injury in C57BL/6 mice. The *in vivo* experiment showed that the pretreatment of fisetin inhibited AST, ALT, IL-1β, IL-6, and TNF-α levels in serum and suppressed the MDA and CAT levels in liver. In addition, fisetin altered the pathological symptoms through macroscopic view and H&E staining. This hepatoprotective effect was possibly related to NF-κB signaling pathway. These findings revealed that flavanols fisetin, quercetin, and myricetin are three potential agents again inflammation disease and among which fisetin might be a promising phytonutrient in the treatment of acute liver injury.

4.2 Outlooks

Besides above results, there are still many limits in this research. Firstly, fisetin was found to be the strongest anti-inflammatory agent compared with quercetin and myricetin. This might be attributed to their minor structure differences. However, how minor structure difference determined different bioactivities effect is unknown. The protein–flavanol interactions should be clarified by structural modeling and X-Ray crystallography to test which site could tightly bind to the important protein involved in inflammation. Secondly, the key target of flavanols (fisetin, quercetin, myricetin) needed to be explored. Quantitative chemoproteomic profiling should be carried out in the future to identify the key target of flavanols. Thirdly, UPLC-MS/MS analysis showed that flavonols were entered the cells quickly and transformed into many forms of metabolites. But how metabolites take functions remains unknown. Further studies

should focus on the relationship between the exact metabolites and the bioactivities. For example, metabolites can be purified or synthesized to detect their bioactivities *in vitro* or *in vivo*.

References

Arai, Y., Watanabe, S., Kimira, M., Shimoi, K., Mochizuki, R., Kinae, N., 2000. Dietary intakes of flavonols, flavones and isoflavones by Japanese women and the inverse correlation between quercetin intake and plasma LDL cholesterol concentration. J Nutr 130, 2243–2250. https://doi.org/10.1093/jn/130.9.2243

Ayala, T.S., Tessaro, F.H.G., Jannuzzi, G.P., Bella, L.M., Ferreira, K.S., Martins, J.O., 2019. High Glucose Environments Interfere with Bone Marrow-Derived Macrophage Inflammatory Mediator Release, the TLR4 Pathway and Glucose Metabolism. Sci Rep 9, 11447. https://doi.org/10.1038/s41598-019-47836-8

Bai, X., Yang, P., Zhou, Q., Cai, B., Buist-Homan, M., Cheng, H., Jiang, J., Shen, D., Li, L., Luo, X., Faber, K.N., Moshage, H., Shi, G., 2017. The protective effect of the natural compound hesperetin against fulminant hepatitis in vivo and in vitro. Br J Pharmacol 174, 41–56. https://doi.org/10.1111/bph.13645

Barreca, D., Trombetta, D., Smeriglio, A., Mandalari, G., Romeo, O., Felice, M.R., Gattuso, G., Nabavi, S.M., 2021. Food flavonols: Nutraceuticals with complex health benefits and functionalities. Trends in Food Science & Technology, Plant-Based Bioactive Compounds: Healthy Promoters And Protective Agents 117, 194–204. https://doi.org/10.1016/j.tifs.2021.03.030

Buchanan, M.M., Hutchinson, M., Watkins, L.R., Yin, H., 2010. Toll-like receptor 4 in CNS pathologies. J Neurochem 114, 13–27. https://doi.org/10.1111/j.1471-4159.2010.06736.x

Chen, X., Shen, J., Zhao, J.-M., Guan, J., Li, W., Xie, Q.-M., Zhao, Y.-Q., 2020. Cedrol attenuates collagen-induced arthritis in mice and modulates the inflammatory response in LPS-mediated fibroblast-like synoviocytes. Food Funct 11, 4752–4764. https://doi.org/10.1039/d0fo00549e

Chen, Y., Ji, N., Pan, S., Zhang, Z., Wang, R., Qiu, Y., Jin, M., Kong, D., 2017. Roburic Acid Suppresses NO and IL-6 Production via Targeting NF-κB and MAPK Pathway in RAW264.7 Cells. Inflammation 40, 1959–1966. https://doi.org/10.1007/s10753-017-0636-z

Chenxu, G., Xianling, D., Qin, K., Linfeng, H., Yan, S., Mingxin, X., Jun, T., Minxuan, X., 2021. Fisetin protects against high fat diet-induced nephropathy by inhibiting inflammation and oxidative stress via the blockage of iRhom2/NF-κB signaling. Int Immunopharmacol 92, 107353. https://doi.org/10.1016/j.intimp.2020.107353

Cutolo, M., Soldano, S., Contini, P., Sulli, A., Seriolo, B., Montagna, P., Brizzolara, R., 2013. Intracellular NF-kB-decrease and IKBα increase in human macrophages following CTLA4-Ig treatment. Clin Exp Rheumatol 31, 943–946.

Feng, L., Zhou, J., Zhang, L., Liu, P., Zheng, P., Gao, S., Song, C., Yu, Y., Gong, Z., Wan, X., 2021. Gut microbiota-mediated improvement of metabolic disorders by Qingzhuan tea in high fat diet-fed mice. Journal of Functional Foods 78, 104366. https://doi.org/10.1016/j.jff.2021.104366

Furman, D., Campisi, J., Verdin, E., Carrera-Bastos, P., Targ, S., Franceschi, C., Ferrucci, L., Gilroy, D.W., Fasano, A., Miller, G.W., Miller, A.H., Mantovani, A., Weyand, C.M., Barzilai, N., Goronzy, J.J., Rando, T.A., Effros, R.B., Lucia, A., Kleinstreuer, N., Slavich, G.M., 2019. Chronic inflammation in the etiology of disease across the life span. Nat Med 25, 1822–1832. https://doi.org/10.1038/s41591-019-0675-0

Gilroy, D.W., Lawrence, T., Perretti, M., Rossi, A.G., 2004. Inflammatory resolution: new opportunities for drug discovery. Nat Rev Drug Discov 3, 401–416. https://doi.org/10.1038/nrd1383

Guo, W., Xiang, Q., Mao, B., Tang, X., Cui, S., Li, X., Zhao, J., Zhang, H., Chen, W., 2021. Protective Effects of Microbiome-Derived Inosine on Lipopolysaccharide-Induced Acute Liver Damage and Inflammation in Mice via Mediating the TLR4/NF-κB Pathway. J. Agric. Food Chem. 69, 7619–7628. https://doi.org/10.1021/acs.jafc.1c01781

Häkkinen, S.H., Kärenlampi, S.O., Heinonen, I.M., Mykkänen, H.M., Törrönen, A.R., 1999. Content of the flavonols quercetin, myricetin, and kaempferol in 25 edible berries. J Agric Food Chem 47, 2274–2279. https://doi.org/10.1021/jf9811065

Hishinuma, I., Nagakawa, J., Hirota, K., Miyamoto, K., Tsukidate, K., Yamanaka, T., Katayama, K., Yamatsu, I., 1990. Involvement of tumor necrosis factor-alpha in development of hepatic injury in galactosamine-sensitized mice. Hepatology 12, 1187–1191. https://doi.org/10.1002/hep.1840120518

Hollman, P.C.H., 2004. Absorption, Bioavailability, and Metabolism of Flavonoids. Pharmaceutical Biology 42, 74–83. https://doi.org/10.3109/13880200490893492

Hu, T.-Y., Ju, J.-M., Mo, L.-H., Ma, L., Hu, W.-H., You, R.-R., Chen, X.-Q., Chen, Y.-Y., Liu, Z.-Q., Qiu, S.-Q., Fan, J.-T., Cheng, B.-H., 2019. Anti-inflammation action of xanthones from Swertia chirayita by regulating COX-2/NF-κB/MAPKs/Akt signaling pathways in RAW 264.7 macrophage cells. Phytomedicine 55, 214–221. https://doi.org/10.1016/j.phymed.2018.08.001

Huang, G.-J., Huang, S.-S., Deng, J.-S., 2012. Anti-inflammatory activities of inotilone from Phellinus linteus through the inhibition of MMP-9, NF-κB, and MAPK activation in vitro and in vivo. PLoS One 7, e35922. https://doi.org/10.1371/journal.pone.0035922

Hwang, J.H., Ma, J.N., Park, J.H., Jung, H.W., Park, Y.-K., 2019. Anti-inflammatory and antioxidant effects of MOK, a polyherbal extract, on lipopolysaccharide-stimulated RAW 264.7 macrophages. Int J Mol Med 43, 26–36. https://doi.org/10.3892/ijmm.2018.3937

Ji, Y., Dai, Z., Sun, S., Ma, X., Yang, Y., Tso, P., Wu, G., Wu, Z., 2018. Hydroxyproline Attenuates Dextran Sulfate Sodium-Induced Colitis in Mice: Involvment of the NF-κB Signaling and Oxidative Stress. Mol Nutr Food Res 62, e1800494. https://doi.org/10.1002/mnfr.201800494

Jo, I.-J., Bae, G.-S., Choi, S.B., Kim, D.-G., Shin, J.-Y., Seo, S.-H., Choi, M.-O., Kim, T.-H., Song, H.-J., Park, S.-J., 2014. Fisetin attenuates cerulein-induced acute pancreatitis through down regulation of JNK and NF-κB signaling pathways. European Journal of Pharmacology 737, 149–158. https://doi.org/10.1016/j.ejphar.2014.05.018

Kandemir, K., Tomas, M., McClements, D.J., Capanoglu, E., 2022. Recent advances on the improvement of quercetin bioavailability. Trends in Food Science & Technology 119, 192–200. https://doi.org/10.1016/j.tifs.2021.11.032

Khan, H.U., Aamir, K., Jusuf, P.R., Sethi, G., Sisinthy, S.P., Ghildyal, R., Arya, A., 2021. Lauric acid ameliorates lipopolysaccharide (LPS)-induced liver inflammation by mediating TLR4/MyD88 pathway in Sprague Dawley (SD) rats. Life Sciences 265, 118750. https://doi.org/10.1016/j.lfs.2020.118750

Lim, H., Park, J.-Y., Abekura, F., Choi, H., Kim, H.-D., Magae, J., Chang, Y.-C., Lee, Y.-C., Kim, C.-H., 2021. 4-O-methylascochlorin attenuates inflammatory responses induced by lipopolysaccharide in RAW 264.7 macrophages. Int Immunopharmacol 90, 107184. https://doi.org/10.1016/j.intimp.2020.107184

Linde, A., Mosier, D., Blecha, F., Melgarejo, T., 2007. Innate immunity and inflammation--New frontiers in comparative cardiovascular pathology. Cardiovasc Res 73, 26–36. https://doi.org/10.1016/j.cardiores.2006.08.009

Linghu, K.-G., Ma, Q.S., Zhao, G.D., Xiong, W., Lin, L., Zhang, Q.-W., Bian, Z., Wang, Y., Yu, H., 2020. Leocarpinolide B attenuates LPS-induced inflammation on RAW264.7 macrophages by mediating NF-κB and Nrf2 pathways. European Journal of Pharmacology 868, 172854. https://doi.org/10.1016/j.ejphar.2019.172854

Liu, H., Zhang, W., Dong, S., Song, L., Zhao, S., Wu, C., Wang, X., Liu, F., Xie, J., Wang, J., Wang, Y., 2015. Protective effects of sea buckthorn polysaccharide extracts against LPS/d-GalN-induced acute liver failure in mice via suppressing TLR4-NF-κB signaling. J Ethnopharmacol 176, 69–78. https://doi.org/10.1016/j.jep.2015.10.029

Liu, S.F., Malik, A.B., 2006. NF-kappa B activation as a pathological mechanism of septic shock and inflammation. Am J Physiol Lung Cell Mol Physiol 290, L622–L645. https://doi.org/10.1152/ajplung.00477.2005

Malayil, D., House, N.C., Puthenparambil, D., Job, J.T., Narayanankutty, A., 2020. Borassus flabellifer haustorium extract prevents pro-oxidant mediated cell death and LPS-induced inflammation. Drug Chem Toxicol 1–7. https://doi.org/10.1080/01480545.2020.1858854

Pan, C.-W., Zhou, G.-Y., Chen, W.-L., Zhuge, L., Jin, L.-X., Zheng, Y., Lin, W., Pan, Z.-Z., 2015. Protective effect of forsythiaside A on lipopolysaccharide/d-galactosamine-induced liver injury. Int Immunopharmacol 26, 80–85. https://doi.org/10.1016/j.intimp.2015.03.009

Park, H.-J., Kim, I.-T., Won, J.-H., Jeong, S.-H., Park, E.-Y., Nam, J.-H., Choi, J., Lee, K.-T., 2007. Anti-inflammatory activities of ent-16alphaH,17-hydroxy-kauran-19-oic acid isolated from the roots of Siegesbeckia pubescens are due to the inhibition of iNOS and COX-2 expression in RAW 264.7 macrophages via NF-kappaB inactivation. Eur J Pharmacol 558, 185–193. https://doi.org/10.1016/j.ejphar.2006.11.036

Peng, H.-L., Huang, W.-C., Cheng, S.-C., Liou, C.-J., 2018. Fisetin inhibits the generation of inflammatory mediators in interleukin-1β-induced human lung epithelial cells by suppressing the NF-κB and ERK1/2 pathways. Int Immunopharmacol 60, 202–210. https://doi.org/10.1016/j.intimp.2018.05.004

Pham, T.-H., Kim, M.-S., Le, M.-Q., Song, Y.-S., Bak, Y., Ryu, H.-W., Oh, S.-R., Yoon, D.-Y., 2017. Fargesin exerts anti-inflammatory effects in THP-1 monocytes by suppressing PKC-dependent AP-1 and NF-κB signaling. Phytomedicine 24, 96–103. https://doi.org/10.1016/j.phymed.2016.11.014

Qian, X.-H., Song, X.-X., Liu, X.-L., Chen, S., Tang, H.-D., 2021. Inflammatory pathways in Alzheimer's disease mediated by gut microbiota. Ageing Res Rev 68, 101317. https://doi.org/10.1016/j.arr.2021.101317

Ren, Q., Guo, F., Tao, S., Huang, R., Ma, L., Fu, P., 2020. Flavonoid fisetin alleviates kidney inflammation and apoptosis via inhibiting Src-mediated NF-κB p65 and MAPK signaling pathways in septic AKI mice. Biomedicine & Pharmacotherapy 122, 109772. https://doi.org/10.1016/j.biopha.2019.109772

Shen, M., Cao, Y., Jiang, Y., Wei, Y., Liu, H., 2018. Melatonin protects mouse granulosa cells against oxidative damage by inhibiting FOXO1-mediated autophagy: Implication of an antioxidation-independent mechanism. Redox Biol 18, 138–157. https://doi.org/10.1016/j.redox.2018.07.004

Smirnova, M.G., Kiselev, S.L., Gnuchev, N.V., Birchall, J.P., Pearson, J.P., 2002. Role of the pro-inflammatory cytokines tumor necrosis factor-alpha, interleukin-1 beta, interleukin-6 and interleukin-8 in the pathogenesis of the otitis media with effusion. Eur Cytokine Netw 13, 161–172.

Stravitz, R.T., Lee, W.M., 2019. Acute liver failure. The Lancet 394, 869–881. https://doi.org/10.1016/S0140-6736(19)31894-X

Surh, Y.J., Chun, K.S., Cha, H.H., Han, S.S., Keum, Y.S., Park, K.K., Lee, S.S., 2001. Molecular mechanisms underlying chemopreventive activities of anti-inflammatory phytochemicals: down-regulation of COX-2 and iNOS through suppression of NF-kappa B activation. Mutat Res 480–481, 243–268. https://doi.org/10.1016/s0027-5107(01)00183-x

Tak, P.P., Firestein, G.S., 2001. NF-kappaB: a key role in inflammatory diseases. J Clin Invest 107, 7–11. https://doi.org/10.1172/JCI11830

Tian, C., Liu, X., Chang, Y., Wang, R., Lv, T., Cui, C., Liu, M., 2021. Investigation of the anti-inflammatory and antioxidant activities of luteolin, kaempferol, apigenin and quercetin. South African Journal of Botany 137, 257–264. https://doi.org/10.1016/j.sajb.2020.10.022

Tian, Y., Zhou, S., Takeda, R., Okazaki, K., Sekita, M., Sakamoto, K., 2021. Anti-inflammatory activities of amber extract in lipopolysaccharide-induced RAW 264.7 macrophages. Biomed Pharmacother 141, 111854. https://doi.org/10.1016/j.biopha.2021.111854

Tu, Y., Wang, K., Wan, J.-B., He, C., 2019. Anti-inflammatory effects of Glycine tabacina extract in LPS-stimulated macrophages and collagen-induced arthritis mice. Journal of Functional Foods 62, 103528. https://doi.org/10.1016/j.jff.2019.103528

Wang, H., Chen, L., Zhang, X., Xu, L., Xie, B., Shi, H., Duan, Z., Zhang, H., Ren, F., 2019. Kaempferol protects mice from d-GalN/LPS-induced acute liver failure by regulating the ER

stress-Grp78-CHOP signaling pathway. Biomedicine & Pharmacotherapy 111, 468–475. https://doi.org/10.1016/j.biopha.2018.12.105

Wang, L., Tu, Y.-C., Lian, T.-W., Hung, J.-T., Yen, J.-H., Wu, M.-J., 2006. Distinctive antioxidant and antiinflammatory effects of flavonols. J Agric Food Chem 54, 9798–9804. https://doi.org/10.1021/jf0620719

Wang, W., Zhang, Y., Li, H., Zhao, Y., Cai, E., Zhu, H., Li, P., Liu, J., 2018. Protective Effects of Sesquiterpenoids from the Root of Panax ginseng on Fulminant Liver Injury Induced by Lipopolysaccharide/d-Galactosamine. J Agric Food Chem 66, 7758–7763. https://doi.org/10.1021/acs.jafc.8b02627

Wang, X., Wang, L., Dong, R., Huang, K., Wang, C., Gu, J., Luo, H., Liu, K., Wu, J., Sun, H., Meng, Q., 2021. Luteolin ameliorates LPS-induced acute liver injury by inhibiting TXNIP-NLRP3 inflammasome in mice. Phytomedicine 87, 153586. https://doi.org/10.1016/j.phymed.2021.153586

Wu, M., Wang, C., Mai, C., Chen, J., Lai, X., He, L., Huang, S., Zhang, X., 2019. Flavonoids from Livistona chinensis fruit ameliorates LPS/D-GalN-induced acute liver injury by inhibiting oxidative stress and inflammation. Journal of Functional Foods 61, 103460. https://doi.org/10.1016/j.jff.2019.103460

Yang, W., Tian, Z.-K., Yang, H.-X., Feng, Z.-J., Sun, J.-M., Jiang, H., Cheng, C., Ming, Q.-L., Liu, C.-M., 2019. Fisetin improves lead-induced neuroinflammation, apoptosis and synaptic dysfunction in mice associated with the AMPK/SIRT1 and autophagy pathway. Food and Chemical Toxicology 134, 110824. https://doi.org/10.1016/j.fct.2019.110824

Yao, D., Shi, W., Gou, Y., Zhou, X., Yee Aw, T., Zhou, Y., Liu, Z., 2005. Fatty acid-mediated intracellular iron translocation: a synergistic mechanism of oxidative injury. Free Radic Biol Med 39, 1385–1398. https://doi.org/10.1016/j.freeradbiomed.2005.07.015

Zhang, C., Li, C., Jia, X., Wang, K., Tu, Y., Wang, R., Liu, K., Lu, T., He, C., 2019. In Vitro and In Vivo Anti-Inflammatory Effects of Polyphyllin VII through Downregulating MAPK and NF-κB Pathways. Molecules 24, E875. https://doi.org/10.3390/molecules24050875

Zhang, L., Chen, J., Liao, H., Li, C., Chen, M., 2020. Anti-inflammatory effect of lipophilic grape seed proanthocyanidin in RAW 264.7 cells and a zebrafish model. Journal of Functional Foods 75, 104217. https://doi.org/10.1016/j.jff.2020.104217

Zhong, R., Farag, M.A., Chen, M., He, C., Xiao, J., 2022. Recent advances in the biosynthesis, structure–activity relationships, formulations, pharmacology, and clinical trials of fisetin. eFood 3, e3. https://doi.org/10.1002/efd2.3

Zhong, Y., Liu, T., Guo, Z., 2012. Curcumin inhibits ox-LDL-induced MCP-1 expression by suppressing the p38MAPK and NF-κB pathways in rat vascular smooth muscle cells. Inflamm Res 61, 61–67. https://doi.org/10.1007/s00011-011-0389-3

Publications

Journal

1. **Zhong RT**[#], Miao LC[#], Zhang HL, Prieto MA, Simal-Gandara J, Chen L, He CW*, Cao H*. Anti-inflammatory activities of flavonols on RAW264.7 macrophages *via* mediating NF-κB and MAPK signaling pathways: Effect of hydroxyl group. *Current Research in Food Science*. (Revision)

2. **Zhong RT**, Farag MA, Chen MW, He CW*, Xiao JB*. Recent advances in the biosynthesis, structure–activity relationships, formulations, pharmacology, and clinical trials of fisetin. *eFood*, 3, 1-2, e3. https://doi.org/10.1002/efd2.3

3. Miao LC, Zhang HL, Cheong MC, **Zhong RT**, Garcia-Oliveira P, Prieto MA, Cheng KW, Wang MF, Cao H, Nie SP, Simal-Gandara J, Cheang WS*, Xiao JB*. Anti-diabetic potential of apigenin, luteolin, and baicalein via partially activating PI3K/Akt/Glut-4 signaling pathways in insulin-resistant HepG2 cells. *Food Science and Human Wellness*. (Accepted).

Conference abstract

1. **Zhong RT**, Xiao JB. Exploration of molecular mechanism of fisetin for cancer chemopreventive potential. *Free Radical Biology and Medicine*. 2022, 180(S1), s39.

Oral presentation

1. **Zhong RT**. 5th International Symposium on Phytochemicals in Medicine and Food. (Nanchang, China; Oct 18-20, 2021). (*Outstanding Master Student's Oral Presentation*)

Poster presentation

1. **Zhong RT**. 5th International Symposium on Phytochemicals in Medicine and Food. (Nanchang, China; Oct 18-20, 2021). (*Best Poster Award*)

2. **Zhong RT**. SfRBM 2021 Virtual Conference. (November 15-18, 2021).